

The Quadrotor Platform

from a military point of view

Mathias Wannberg

mwan@kth.se

7/2/2012

Abstract

The use of military UAV's has become increasingly popular amongst the military powers of the world. But most of these UAV's lack the vertical take-off and landing (VTOL) ability. This report investigates the quadrotor which is an excellent VTOL platform. The main disadvantage that the quadrotor platform possesses is that it suffers from poor performance if compared to airplanes. Quadrotors lack the endurance and the capability to carry heavy payloads. An effort is to be done to investigate the possible application area of use for the quadrotor platform from a military point of view. In order to solve these problems, two COTS (Commercial off the Shelf) quadrotors has been bought and a number of test flights have been performed with them. The results from these tests have been evaluated in *MATLAB* and a number of simulation models have been created in order to get a clear picture of the quadrotors potential. Rotorcraft such as the quadrotor is affected by the aerodynamic phenomena of induced power, this phenomena is important to understand when designing a control system for the quadrotor and when optimizing its endurance. A number of suggestions for how to improve the quadrotor platform have been proposed such as using ducted propellers, hybrid fuel systems, gyroscopes, and micro technology. A simulation model has been created that predicts the time that a quadrotor of a given size carrying different payloads could maintain itself in hover, this model show that battery based quadrotors are limited in how big they can be made. Much work has been dedicated to the extended sight concept where the quadrotor is intended to be powered by a cable and serve as a pair of extra eyes to an army vehicle such as a tank in an urban environment. Most of the technical difficulties for this concept has been defined and solved, these are mainly electrical difficulties and work on a demonstrator for this concept has been started. All these investigations points towards that the military would benefit from having quadrotors in their arsenal, they could be used for reconnaissance, placing out surveillance equipment and resupplying soldiers behind enemy lines.

Background

This suggested thesis was defined and launched by *Swedish Defense Material Administration (FMV)* in consensus with *Etteplan*. It serves as a continuation to the Pegasus project where it was concluded that a quadrotor platform is the most promising one for the given issues. The course of this thesis was successively altered during the project in consensus with *FMV*.

Table of Contents

1. Introduction.....	7
1.1 History	7
2. Aerodynamic effects	9
2.1 Thrust dependence.....	9
2.2 Blade flapping.....	11
3. Reverse-engineering and testing of a quadrotor	12
3.1 AR.Drone technical specifications	12
3.2 Flight performance.....	13
3.2.1 Discussion of flight performance results.....	14
3.3 Efficiency	15
3.3.1 Adding a duct to the propulsion system	18
3.4 Flying the AR.Drone out of sight.....	20
3.4.1 The test	20
4. Military benefits	22
4.1 Short range supply	22
4.2 Extended sight ("utflyttbart sikte"[in Swedish])	22
4.2.1 The cable	22
4.2.2 DC-system	25
4.2.3 Extended sight – Ground forces version	26
4.2.4 Extended sight – Tank version.....	27
4.2.5 High voltage systems	27
4.2.6 Aerodynamic forces acting on the cable	27
4.2.7 Alternative to the quadrotor platform.....	29
4.2.8 Extended sight flight strategy.....	30
4.3 Flight strategies	31
5. Sizing effects	32
5.1 Square-cube law.....	32
5.2 Engines.....	32
5.3 Rotor size	32
5.4 Agility with scaling	33
6. Flight time approximation model	35
6.1 Mass model	35
6.1.1 Propeller mass	35
6.1.2 Engine mass	35
6.1.3 Structure mass	35
6.1.4 Miscellaneous mass	36
6.2 Efficiency	36
6.3 Energy density.....	36
6.3.1 Li-Po.....	36
6.3.2 Hybrid system.....	43
7. Extended sight - Demonstrator	47
7.1 Electrical system.....	47
7.1.1 Testing the electrical system	48
7.2 Flying the AR.Drone tethered	49
8. Conclusion	52

9. Recommendations for future work	53
9.1 Ducted fan quadrotor	53
9.2 Finalize and test the extended sight demonstrator	53
9.3 Build MW-8R	53
9.4 Gyroscopes potential	53
9.5 Efficiency of propellers and engines	54
9.6 Evasive maneuver programming	54
9.7 Indoor reconnaissance programming	54
10. References	55
11. Appendix	56
11.1 Appendix A – Propeller theory	56
11.2 Appendix B – AR.Drone system specifications	58
11.3 Appendix C – AR.Drone propulsion system test	59
11.4 Appendix D – AR.Drone ducted fan measurements	61

Nomenclature

P	Power [W]	α_0	Temperature coefficient [$1/^\circ$]
T	Thrust [N]	T_c	Temperature in cable [$^\circ$]
W	Weight of aircraft [N]	T_0	Temperature of surrounding air [$^\circ$]
T_h	Thrust required to hover [N]	$\rho_r(T)$	Resistivity as function of temperature [Ω]
V	Free stream velocity [m/s]	ΔU	Potential drop in cable [V]
v_h	Induced wind speed [m/s]	V_{source}	Potential of the source [V]
T_h	Thrust required to maintain hover [N]	V_{quad}	Potential over quadrotor [V]
ϱ	Density of air [kg/m^3]	m_{cable}	Cable mass [kg]
S	Rotor swept area [m^2]	ρ_{metal}	Density of metal [kg/m^3]
v_i	Induced wind speed [m/s]	$I_{1:1}$	MOI - full scale system [kgm^2]
α	Angle of attack [$^\circ$]	$I_{1:2}$	MOI- half scale system [kgm^2]
n_i	Efficiency of component i [–]	r	Distance to point mass [m]
ρ_r	Resistivity [Ωm]	m_p	Propeller mass [kg]
P_{loss}	Power loss in cable [W]	v	Propeller volume [m^3]
R_{cable}	Resistance of the cable [Ω]	r_p	Propeller radius [m]
L	Length of cable [m]	ρ	Propeller density [kg/m^3]
A	Cable cross sectional area [m^2]	m_e	Mass of engine [kg]
\emptyset	Diameter of the cable [m]	E_d	Energy density [Wh/kg]
I	Current [A]	m_b	Mass of batteries [kg]
ΔT	Temperature increase in cable [$^\circ$]	r_t	Tube radius [m]
A_m	Cable mantle area [m^2]	A_p	Projected area perpendicular to the wind [m^2]
Q	Heat conductance [W/m^2]	C_d	Drag coefficient [m]
ϱ	Density of air [kg/m^3]	$R_{1,2}$	Reaction force [N]
ρ_0	Resistivity at room temperature [Ωm]	θ	Angle between quadrotor and cable [$^\circ$]

Acknowledgements

The author would like to thank his mentor Owe Lyrsell for all his useful help given in the technical difficulties and for constantly steering the project into the right direction. He would also like to thank Erik Prisell at *Swedish Defense Material Administration* for his useful derivations of aerodynamic propeller equations. The author would also like to thank Tomas Leijon at *Airspeed Industry* for sharing his experience in radio controlled aircraft and Professor Arne Karlsson at *KTH* for being his mentor at the university.

1. Introduction

Quadrotor helicopters are an increasingly popular rotorcraft concept for unmanned aerial vehicles (UAV). The aircraft consist of four rotors in total placed on the corners of an imaginary square, with two of the rotors counter-rotating thus eliminating the yaw moment produced by the rotors. Quadrotor hovercraft possesses two main advantages over conventional helicopters. First, quadrotors do not require the complex mechanical rotor linkages for rotor actuation, relying instead on fixed pitch rotors using variation on motor speed for vehicle control. Second, since quadrotors use four smaller rotors than a helicopter of the same weight, less kinetic energy is stored in the rotors thus reducing the risk for damage if they should encounter any objects. A quadrotor require however a quite complex electrical control system based on gyroscopes and microprocessors. The recent increase in popularity for the quadrotor platform is largely due to the reduction in price for these components. This work focuses on the quadrotor concept from a military point of view. Investigations of the military benefits of such an aerial vehicle are to be done and based on these, different quadrotor concepts is to be studied. In order to keep the costs down, a COTS quadrotor is to be used as a reference to investigate the possible military potential of the quadrotors found on the civil market. A quadrotor called AR.Drone manufactured by *parrot* is going to be reverse-engineered to get a better understanding of its military potential. The quadrotor is also to be used as a tool to verify and test different concepts.

1.1 History

Quadrotors where among the first successful heavier than air VTOL vehicles in the 1920's, but have since then been used very scarcely. The first prototype of a quadrotor appeared 1920 by a scientist called Etienne Oemichen. This first design failed the initial attempt to become airborne but after some calculations and redesigns Oemichen was able to come up with a design that was actually capable of lift off and his prototype even established a world record for helicopters in 1923, remaining airborne for up to 14 minutes. Another early designer of a quadrotors was George De Bothezat, he's quadrotor was designed to take a payload of three people in addition to the pilot and was supposed to reach an altitude of 100 meters, but it was only capable of 5.

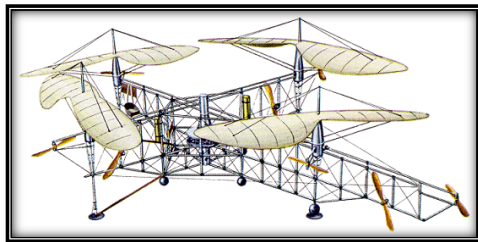


Figure 1- Etienne Oemichen, 1922

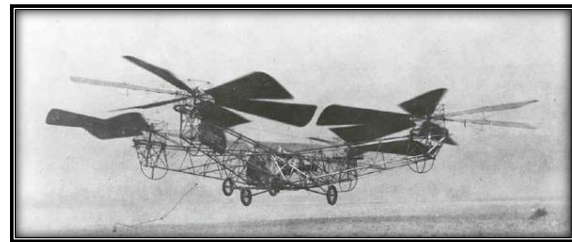


Figure 2 - George De Bothezat, 1923

Both Oemichen and Bothezat designs were propelled by propellers perpendicular to the main rotors and where therefore not true quadrotors. Since these early designs suffered from poor engine performance and could only reach a couple of meters in height, not much was done to the quadrotor design during the following three decades. It was not until the mid-1950's the first true quadrotor flew, which was designed by Marc Adman Kaplan. He's quadrotor design, Convertawings Model "A", first flew 1956 and did so with great success. The 1 ton heavy quadrotor was able to hover and maneuver using its two 90 horsepower engines. Control for this quadrotor did not require additional propellers perpendicular to the main rotors, but was obtained by varying the thrust of the main rotors instead. Even though this design flew successfully, people saw little interest in the quadrotor since they required heavy pilot workload and could not compete with the performance specifications of conventional aircraft such as speed, payload, range, and endurance.

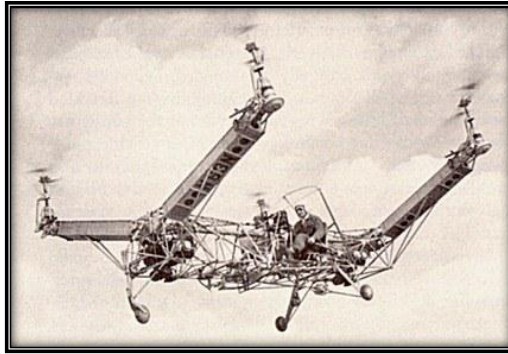


Figure 3 - Marc Adam Kaplan, 1956

These days the quadrotor platform is widely used in the UAV business, mostly used to take aerial pictures/videos and for surveillance. One of the most advanced quadrotors on the market is *Microdrones md4-1000* that is capable of flying up to 60 *minutes* with a payload of 500 *grams*.



Figure 4 - Microdrones md4-1000

The future of the quadrotor platform seems bright; Vijay Kumar is a professor at the University of Pennsylvania that is currently doing research on autonomous quadrotor systems. His quadrotors are able to autonomously enter and fly through an unknown building while creating a map of it. They are also capable of complex formation flight and of constructing simple cubic constructions autonomously.



Figure 5 - Vijay Kumar's quadrotors performing formation flight

2. Aerodynamic effects

The quadrotor platform is fairly easy to control in hover with the aid of onboard computers, but when a quadrotor is flying in translational flight this change. This is mainly caused by the aerodynamic effect of thrust variation due to power induced in the rotors, but blade flapping due to different effective airspeed on the advancing and retreating blade caused by the free-stream velocity could also degrade controls. The thrust variation phenomena have a large impact on altitude control while blade flapping can in some cases have an effect on the attitude control.

2.1 Thrust dependence

Just like a wing the rotor gains lift with higher α , and increased mass flow through the rotor results in an effect called translational lift. A quadrotors lift can be analyzed as for a helicopter, and the calculations should be done for one rotor at the time, with a fourth of the quadrotors total weight as input parameter, this weight is denoted as T_h .

At hover, the free stream velocity is zero; this means that the equation used to describe the thrust to power ratio for aircraft propellers gives zero force at a given power input, which is obviously not true.

$$P = T \cdot V \quad (1)$$

The rotor in hover sees no free stream velocity, but the rotor induces a wind by sucking in the air around the rotor. This is called the induced wind speed at hover. Using Newton's second law of motion and the knowledge that the slipstream velocity is two times larger than the induced velocity at the rotor disc, one can derive an expression for the induced velocity. This is done in Swedish by aerospace engineer Erik Prisell and is presented in Appendix A.

$$v_h = \sqrt{\frac{T_h}{2\rho S}} \quad (2)$$

Where ρ is the density of the air and S is the area swept out of the rotor blades. Inserting equation (2) in (1) yields an expression for the power required to hover.

$$P_h = \frac{T_h^{3/2}}{\sqrt{2\rho S}} \quad (3)$$

In translational flight, the rotor disc also induces a velocity through as for in hover. This velocity v_i is expressed by equation (4) which was originally derived by Glauert in the mid 1920's [1].

$$v_i = \frac{v_h^2}{\sqrt{(v_\infty \cos \alpha)^2 + (v_i - v_\infty \sin \alpha)^2}} \quad (4)$$

Where α is defined as the geometric angle between the free stream velocity v_∞ and the rotor plane where positive values of α corresponds to pitching up with respect to the free stream velocity. Solving this fourth degree polynomial equation for v_i for fixed values on α and v_∞ , and known value on v_h , yields the induced velocity which is used to compute the power required for translational flight.

$$P = T \cdot (v_i - v_\infty \sin \alpha) \quad (5)$$

Using equations (3) & (5) makes it possible to compute a quota between the power required to obtain the thrust $T = T_h$ in translational flight and the power required to produce the same thrust in hover. The magnitude of this thrust is set to be the thrust required to keep the aircraft in hover, $T = T_h$, in order to get a feeling of how much energy that needs to be spent in translational flight compared to hovering. This ratio is plotted for different fixed values on v_∞ and α and presented in Figure 6.

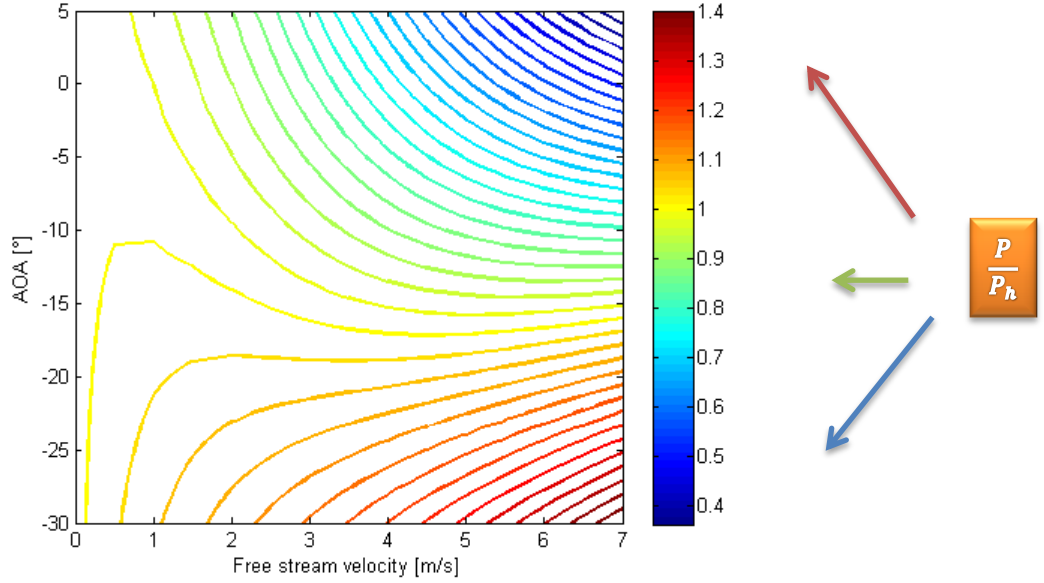


Figure 6 - Power required maintaining the constant thrust $T = T_h$
 $(T_h = 0.981 \text{ N}, \rho = 1.225 \frac{\text{kg}}{\text{m}^3}, S = 0.0312 \text{ m}^2)$

Figure 6 show that the ratio P/P_h depends vanishingly little on a change of the angle of attack at low speeds. But as the speed increases this ratio becomes increasingly sensitive to changes of the angle of attack. Two examples of how to read this graph is presented below this text:

1. If the quadrotor is flying with an angle of attack of 5° at a speed of 6 m/s, the color of the line that is crossing this point in the graph is dark blue, by looking at the color bar to the right of the Figure 6 one can see that dark blue represent a value of 0.4. This means that only 40 % of the power used to produce the same thrust in hover is needed to produce the same force at current flying conditions.
2. If the quadrotor instead is flying with an angle of attack of -27° at a speed of 3 m/s, then the color of the line that is crossing this point in the graph is orange, this represents a value of 1.1 in the color bar. This means that 110 % of the power is needed to produce the same force as in hover.

The quadrotor is able to fly at all of these α and speed, but static horizontal flight is only possible on a line where all the forces affecting the quadrotor are in equilibrium, this line can be seen in Figure 11.

This variation in power to produce the same thrust has to be taken into account when one is designing the control system for a quadrotor.

An example: If the quadrotor is flying with airspeed and suddenly changes its attitude to positive α it would start to loose speed. If the control system does not reduce the thrust due to the induced power effect, the quadrotor would also start to gain altitude since the thrust obtained if using the same power input could easily become twice the size when suddenly changing the attitude of the quadrotor due to maneuvering.

In order for one to be able to determine the induced power in horizontal flight, which should be seen as all values of the ratio $P/P_h < 1$, one has to make sure that the vertical component of the thrust vector equals to the weight of the quadrotor. This means that the thrust that the rotor is required to produce increases when α is increased or decreased. The thrust required is now:

$$T_{horizontal} = \frac{T_h}{\cos(\alpha)} \quad (6)$$

This thrust is used in equation (5) and a new quota between the total thrust and the thrust required to hover is computed for different α and v_∞ . Figure 7 shows how the induced power depends on α and v_∞ for the AR.Drone in horizontal flight (which uses the same values on T_h , S , and ρ as in Figure 6).

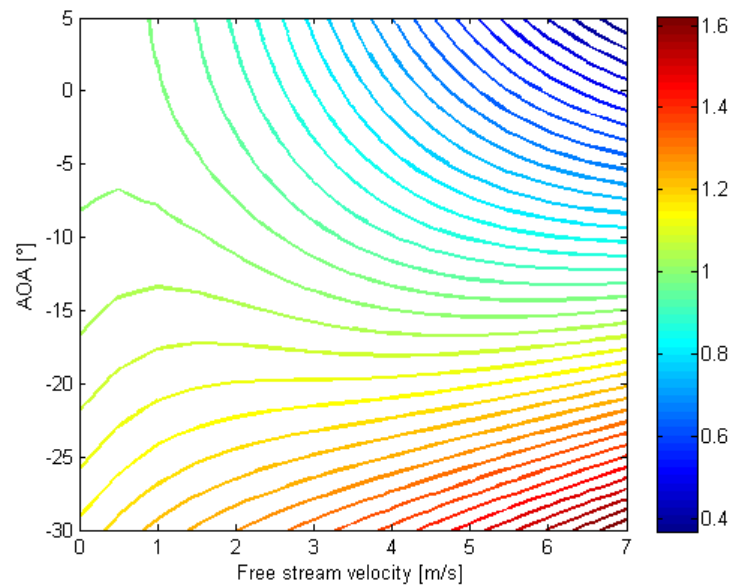


Figure 7 – Power required in horizontal flight

2.2 Blade flapping

A rotor in translational flight undergoes an effect known as blade flapping. The advancing blade of the rotor has a higher effective wind speed than the retreating blade relative to the free-stream velocity. This causes an asymmetry in lift, and results in an up and down oscillation of the rotor blades as shown in Figure 8. If the rotor plane is not aligned with the center of gravity, a moment around C.G is also created due to the blade flapping that further complicates attitude control. This effect might be negligible since the quadrotors rotors could be running on an overcritical frequency which means that the asymmetry in lift is changing with such a high frequency that it does not affect the dynamics of the quadrotor. But further analysis of this phenomenon is beyond the scope of this report but the reader should now that this effect could degrade the performance of the attitude control.

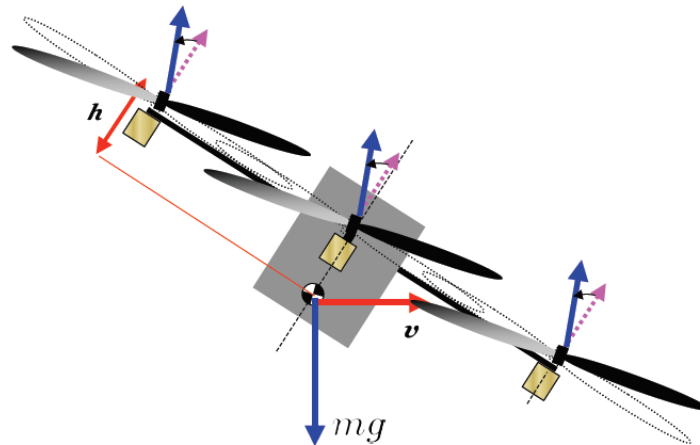


Figure 8 - Effect of blade flapping in forward flight

3. Reverse-engineering and testing of a quadrotor

In order to get a better understanding of the performance of COTS quadrotors, a quadrotor called AR.Drone manufactured by the company *parrot* is to be reverse-engineered. The information gained from this study is to be used to get a better understanding of the full potential of the aircraft and how it could be improved.



Figure 9 - AR.Drone

The AR.Drone quadcopter uses accelerometers and gyroscopes on all of its principal axes to measure accelerations and attitude variations. With this information and the information gathered from an ultrasound altitude meter the onboard computer system autonomously manages to hold the aircraft in a static hover. The vehicle is controlled by smartphones with embedded accelerometers using the Wi-Fi network. Leaning the smartphone in one direction will make the AR.Drone fly in the same direction. The AR.Drone also has an embedded video camera that streams live video from the aircraft to the smartphone, and its open source firmware makes the aircraft popular as a platform for homebuilders and all kinds of master thesis on universities around the globe.

A lot of activity related to the AR.Drone is available on the online forums and one of the users on the forum has created a computer based diagnostics tool called *AR.Drone Diagnostics*. This is a free program that has the ability to control and monitor the quadcopter from a computer. The maximum range of which the aircraft can be controlled could also be extended by using this program and a strong Wi-Fi transmitter on the computer. The program receives data from the sensors of the quadrotor every 3 ms, around 150 different values can be analyzed live during flight or saved to a file and analyzed later. Using these data the user can easily plot variables such as engine rpm, altitude, accelerations, and attitude.

3.1 AR.Drone technical specifications

In this report the flight performance of the AR.Drone quadcopter is sometimes presented in three different configurations of the aircraft:

1. AR.Drone with indoor hull
2. AR.Drone with outdoor hull
3. AR.Drone without hulls

Table 1 contains some important weight and dimension data for the quadcopter.

Configuration	Mass [g]	Dimension [cm]
AR.Drone [1]	427	52.5 x 51.5
AR.Drone [2]	404	45.5 x 45.5
AR.Drone [3]	372	45.5 x 45.5
Battery	102	7 x 4

Table 1 – Mass and size data

The aircraft contains a set of subsystems, the technical specifications of them is presented in Appendix B.

3.2 Flight performance

This section will focus on the flight performance of the AR.Drone.

Before any serious flight testing could begin, an investigation if the two different hulls affected the total time the aircraft could remain in hover was executed. This was done since the indoor hull somewhat resembles a ducted fan propeller system and these are more efficient in hovering conditions. Weights were added on the outdoor configuration to equal the total weight of the indoor configuration and flight testing is done by using the same battery pack since these are individuals. The results from this test showed that there is no difference between the two hulls.

The total time each configuration could maintain hover until the batteries are empty, is presented in Table 2. Note that all test flight is performed at an altitude of 1.5 m to avoid the ground effect.

Configuration	Time
AR.Drone [3]	12 min
AR.Drone [2]	10 min 50 s
AR.Drone [1]	10 min 28 s

Table 2 - Flight times in hover

The current required to hover at different weight loads are presented in Table 3, note that the “parasitic” current of 0.211 A from the onboard electrical system with video camera and Wi-Fi has not been subtracted from presented values.

Mass [g]	I_{tot} [A]
372	4.8
404	5.35
440	5.95
472	6.3
495	6.7
510	6.85
535	7.2

Table 3 - Mass vs. Current

The program that controls the AR.Drone during its flight enables the user to limit the maximum α that the aircraft is allowed to fly at. A test was done at an indoor football arena where the AR.Drone [1] was flown horizontally at different fixed values of α , the distance of the football field was known and by taking the time that it took for the quadrotor to fly this distance one could calculate at what speed the aircraft was flying with for every α . Corresponding speed and theoretical induced power is presented in Table 4. Negative values on the induced power means that more power is needed to maintain horizontal flight.

α [°]	Speed [m/s]	Power required [-]
-5	1.47	0.978
-10	2.87	0.957
-12	3.30	0.967
-15	3.89	1.01
-20	4.96	1.137
-25	5.19	1.302

Table 4 - Speed vs. angle of attack

The maximum takeoff weight for the aircraft is 652 g; note that the quadcopter is sluggish in control and unstable in hover at this weight load, the probable cause for it being unstable, is that its center of gravity has changed somewhat when adding weights on the vehicle. Flying with high angle of attack ($\alpha < -27^\circ$) also makes the AR.Drone enough unstable that a crash is often followed as a result of it.

3.2.1 Discussion of flight performance results

Using the data from Table 3 and subtracting the parasitic current of 0.211 A with the knowledge that the system potential is 11.1 V; one can calculate the power consumed by one of the aircrafts rotors. Equation (3) yields the ideal power consumption for one rotor; the quota between the ideal and actual power consumed makes it possible to plot the efficiency of the AR.Drone at different weight loads, which is presented in Figure 10.

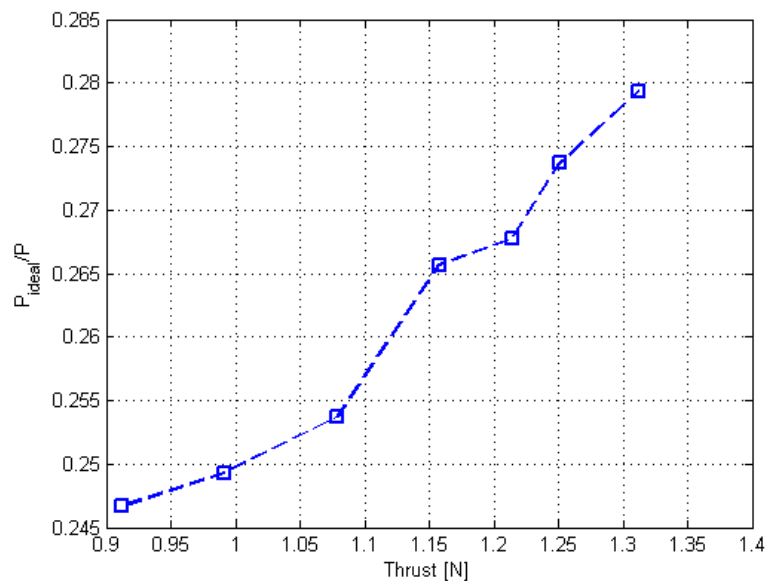


Figure 10 - Efficiency vs. Thrust in hover

One can see that the Quadrotor has a low efficiency. One explanation for this might be that it requires more power to balance the aircraft, since accelerating/decelerating the rotors draws extra current. The next chapter is focused on determining where this loss occurs.

The data from Table 4 show that AR.Drone benefits slightly from the induced power in horizontal flight as long as the angle of attack is not lower than approximately -15° , above this limit the induced power becomes negative as for ordinary aero planes, this means that in order to produce the same thrust one needs to put in more electrical power into the engines. This effect explains why the speed increase gained from going to an angle of attack of 25° from 20° is so small compared to going from 5° to 10° along with the fact that the drag force is a function of the speed squared.

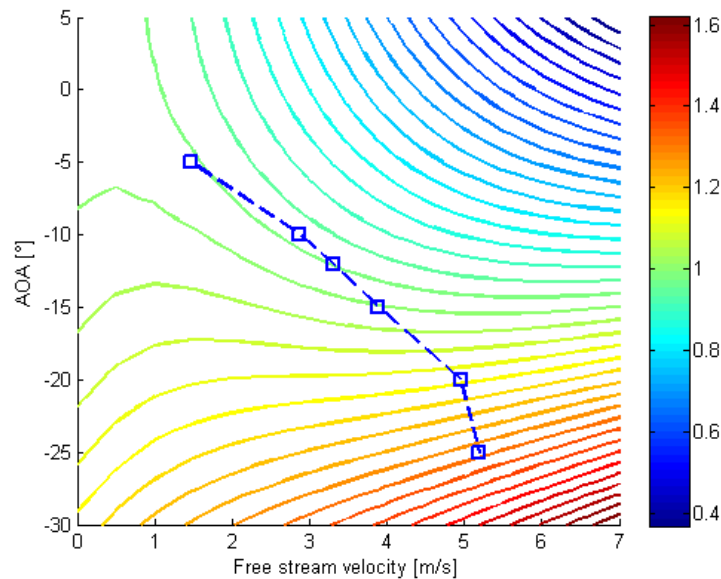


Figure 11 - Induced power in horizontal flight

The blue line in Figure 11 represents where in the induced power graph the quadrotor flies based on the test results presented in Table 4.

The program *AR.Drone Diagnostics* was also tested in flight with good results. It was found out that using *AR.Drone Diagnostics* to control the AR.Drone instead of using smartphones improved maneuverability, using the keyboard inputs to control the quadrotor instead of tilting the smartphone enables the user to perform much more precise and faster maneuvers.

3.3 Efficiency

The low efficiency obtained in the flight performance investigation raised the question of where all this energy is wasted. So an effort is to be done to determine in what components of the quadrotor these losses occurs. It was first thought that the electrical system onboard draw more current in flight and that much of the energy was lost in accelerating the engines in order to balance the quadrotor. Another explanation for the low efficiency could be that the quadrotor platform, with four rotors placed close together on the corners of a square with two of the rotors counter rotating in some way dissipated the thrust generated from the rotors. The above mentioned possible sources of dissipation of energy and the obvious source of loss from the engine, propeller and its gearwheel was tested by ordering a thrust to energy test from the company *Airspeed Industry*. It was practical to test the efficiency of the propulsion system which can be seen in Figure 12.



Figure 12 – AR.Drone propulsion system

This was done by putting the engine with its propeller and corresponding gearwheel on a scale and measuring the thrust obtained for different power inputs. The results and more thoroughly details from this test appear in Appendix C. This test gives a value for the efficiency of the engine, propeller and gearbox combined.

$$\eta_{engine} \cdot \eta_{gearwheel} \cdot \eta_{propeller} \quad (6)$$

The values obtained from this test are presented in Table 5.

Thrust [N]	Power consumption [W]
0	1.1
0.297	6.05
0.674	12.1
1.059	18.15
1.424	24.2
1.839	30.25
2.172	36.3
2.443	42.35

Table 5 - Thrust vs. Power consumption

Equation (3) is again used to determine the ideal power consumption, the quota between the ideal power and the actual electric power used, determines the efficiency of the system. Note that 1.1 W is subtracted from the measured power consumption at different thrusts when the efficiency of the system is calculated since it can be seen as the parasitic system power consumption. This was also done in the measurement of the efficiency for the quadrotor in hover. Figure 13 shows how efficient the propulsion system is at different thrust levels for both tests.

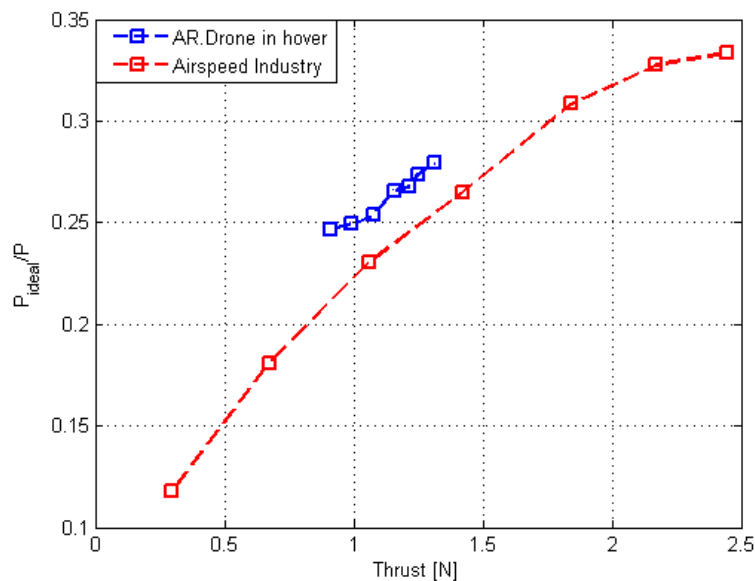


Figure 13 - Airspeed Industry and AR.Drone total efficiency at different thrust levels

The slope of the both efficiency curves has the same magnitude, but the curve for the AR.Drone in hover has slightly higher values of its efficiency. This difference is most probably due to the margin of error between these two tests. The small difference between these two tests can be explained by how the test for the AR.Drone in hover was made. This measurement was done by letting the AR.Drone hover at a height of 1.5 m with a significant heavy cable connected to a multimeter hanging freely in the air to the ground. The weight of the cable was added to the total weight that the quadrotor lifted, but as the quadrotor varied slightly in height this weight was a bit hard to estimate and that is what most likely resulted in the small deviation between the two different tests.

This makes it clear that the only source of energy dissipation is in the propulsion system and not from any of the above stated other possible reasons. But if one is assuming that both tests are accurate, a possible reason for that the quadrotor in hover is more efficient might be that the quadrotor platform as a whole is more efficient than a single propeller.

Since *Airspeed Industry's* test results give the product of the efficiency for the engine, gearwheel and propeller, a brief analysis is done in order to give a hint of how efficient each of the three components are. The efficiency of a brushless engine of the same small size as the current one is about 73 %; this value was obtained by searching the web for efficiency values for engines of similar size. The efficiency of a gearbox is commonly said to be 99 % for every gearwheel. This means that the efficiency of the propeller of the AR.Drone in hover is:

$$n_{propeller} = \frac{n_{hover}}{n_{engine} n_{gearwheel}} = \frac{0.25}{0.73 \cdot 0.99} = 0.346 \quad (7)$$

This seems to be a quite small value since airplane propellers can reach efficiency values of up to 0.8, but this is a small propeller and they tend to get less efficient due to Reynolds number effect and due to poor surface finishing. Equation (8) can be used to estimate the efficiency of propellers that produces static thrust (Appendix A). This expression is based on Bendemann's equation where K is a correction factor due to losses that mainly occur in the propellers slipstream.

$$n_{proptheory} = 1 / \left(\frac{1}{K} \right)^{3/2} \quad (8)$$

Where $K = 0.6$ for lightly loaded propellers and $K = 0.5$ for heavy loaded propellers. The propeller of the AR.Drone can be said to be heavy loaded, the tip of its blades flex significantly when in hover. With this value on K the efficiency is:

$$n_{proptheory} = 1 / \left(\frac{1}{0.5} \right)^{3/2} = 0.354$$

This theoretical value almost matches the calculated value based on the test and estimated values on efficiency of the engine and gearing, since this is the case the value of the calculated efficiency can be seen as a valid number.

The test results raises however another question. Why is the efficiency increasing with higher propeller load? It is known that a higher loaded propeller is less efficient, brushless engine efficiency curves found on the web show that these engines have almost constant efficiency, and the gearing efficiency is a constant. The propeller efficiency is most likely the one that is increasing, this is most likely explained by that the propeller has been optimized to produce thrust well above the thrust required to maintain hover.

3.3.1 Adding a duct to the propulsion system

A duct to the propulsion system was also built in order to compare a ducted fan propeller configuration with the original one. Figure 14 show the AR.Drone with its new duct.



Figure 14 - AR.Drone with its duct

The performance of the ducted fan propeller system was tested in the same way as for the propulsion system without a duct and more thoroughly details from this test is presented in Appendix D. The values obtained from this test are presented in Table 6.

Thrust [N]	Power consumption [W]
0	1.1
0.360	6.05
0.840	12.1
1.213	18.15
1.645	24.2
2.043	30.25
2.493	36.3
2.684	39.3

Table 6 - Thrust vs. Power consumption (ducted fan propeller system)

Figure 15 show the difference in thrust obtained between the ducted fan propeller system and the original propeller system.

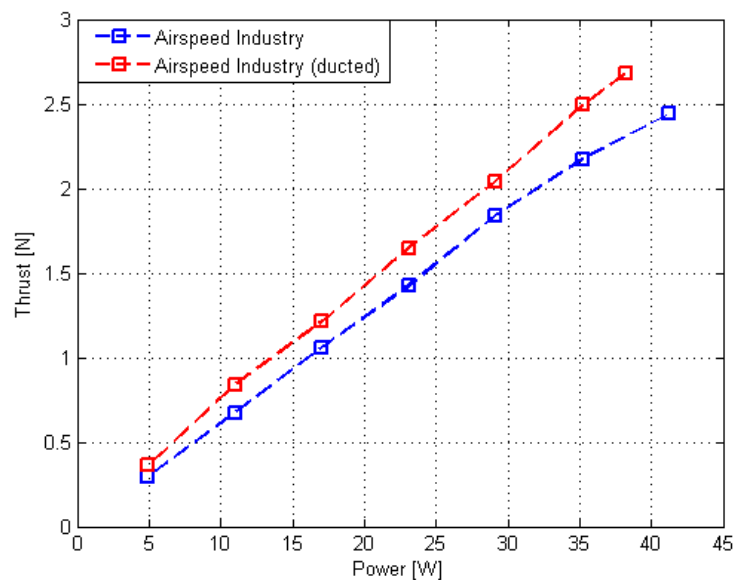


Figure 15 - Ducted fan propeller vs. Propeller

Figure 15 show that the ducted fan system is always performing better than the propeller system. The performance of the ducted fan propeller system is however increasing with higher power inputs, this is explained by the fact that the duct gains more lift when the propeller is drawing air into the duct with a higher velocity, since this lift is proportional to the velocity of the air to the power of two as for ordinary lifting bodies. The difference in the thrust obtained for the two propeller system is quite low however; the ducted fan propeller system is only producing about 15 % more thrust than the propeller when well optimized ducts are claimed to be able to produce up to 90 % more lift than a propeller of the same size in some cases [2]. This means which that the constructed duct is far from optimal and can be improved.

It is not entirely correct to compare a ducted fan propeller system in the efficiency domain for an ordinary propeller since these are two different systems, but if this is done one can see that the ducted fan propeller system designed is about 23 % more efficient than the propeller, if one could design a duct for the quadrotor that produces 90 % more thrust one could increase the efficiency of the system with about 262 % compared to a propeller, this is explained by looking at equation (3) and seeing that the power is depending on the lift that is to be produced to the power of $3/2$, $\left(\frac{T_{h,ducted}}{T_{h,unducted}}\right)^{3/2} = \left(\frac{1.9}{1}\right)^{3/2} = 2.62$. If a duct with this performance could be made, it would dramatically improve the performance of the quadrotor. This means

that a ducted fan quadrotor could in theory maintain itself in hover for almost three times longer than a quadrotor without a duct.

Ducts are generally known to be more efficient in the low speed flight regime, but with higher speed the drag of the duct itself (as a body in the free stream) begins to reduce the total performance of the system. Since quadrotors operate at fairly low speeds this should not be a problem and one could therefore claim that a ducted fan propeller system is to be preferred when designing a quadrotor.

3.4 Flying the AR.Drone out of sight

In order for the military to have any use for a quadrotor for reconnaissance, the quadrotor should be able to fly and operate when out of sight. Most UAV's used for military applications use GPS coordinates and navigates autonomously to each point. This system would however be flown exclusively by the information sent from the video sensors when out of sight. Even though a possible future purpose-built quadrotor for military applications would incorporate an autonomous navigation system, the quadrotor lends itself to applications including flying close to the ground, and even land to have a better look at area and objects intended to be observed. In such a case you must use cameras onboard with a real-time link to the operator to be able to make these adjusted navigations.

The AR.Drone have two cameras onboard, one camera is pointed in the forward direction of the aircraft while the other camera is pointing downwards. The frontal cameras resolution is 640x480 dpi while the downwards have less resolution but provides more frames per second. A test is performed to see how well one can operate an AR.Drone indoors when it is out of sight for the operator.

3.4.1 The test

It was tested how well AR.Drone was able to maneuver and move through doors in the indoor environment of our office. Figure 16 shows the indoor environment and the flight path that the quadrotor flew.

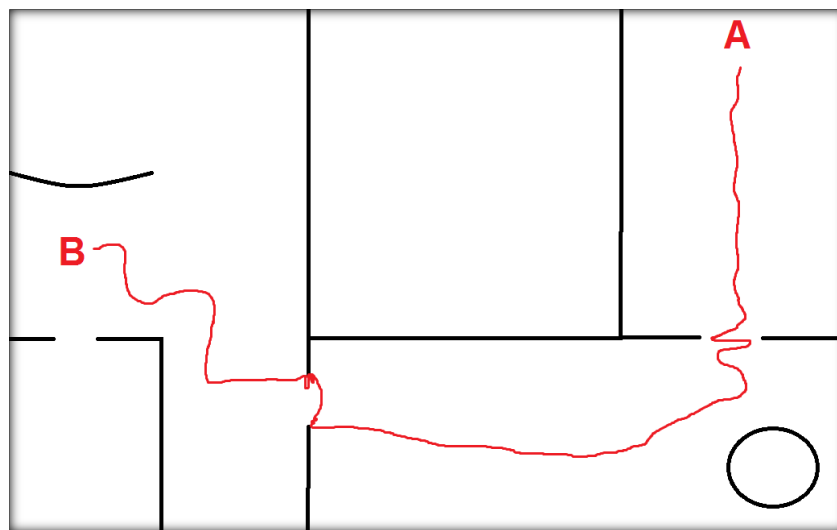


Figure 16 – Indoor environment

As one can see from the flight path in Figure 16, it is hard for the operator to get the AR.Drone through open doors. The quadrotor tend to get stuck or bounce between the walls of the gap before it finally passes through. Without the indoor protection hull (which can be seen mounted on the AR.Drone in Figure 9) it would have been nearly impossible to pass through small passages like door openings without crashing due to propellers hitting the wall.

This test proved that it is possible to fly the AR.Drone exclusively by the information provided by the onboard cameras even though the Wi-Fi link is extremely poor, the poor link often leads to gaps of a few seconds between the video images. The AR.Drone does not however lose control when this happens since it is programmed to stay still in hover at the same altitude, this is an important feature and it would have been nearly impossible to fly the aircraft without it. When the pilot is releasing the controls the AR.Drone also remains in hover at the same altitude where the controls where released, this removes much of the pilot work load and enables the pilot to have time to get familiar with the surroundings. But for a quadrotor to be used for exploration of buildings much need to be done to improve this system since the quadrotor is not able to remain in perfect hover when the controls or Wi-Fi is lost. The quadrotor tends to drift significant

from the position that it is supposed to hold and if it drifts over a chair or an object the height of it is added to the altitude of the quadrotor since the system thinks it has lost this altitude. This altitude increase results sometimes that the quadrotor crashes into the roof of the room.

The video quality is barely sufficient to explore indoor environments but it gives a good understanding of the bigger picture when one is flying in large open areas. An improvement in video quality would help the operator to get a better understanding of the surroundings of an indoor environment and easier obtain the information that the mission requires. Figure 17 & 18 shows the view that the operator of the AR.Drone sees while controlling it.



**Figure 17 – View from AR.Drone in flight
(not from the test)**



**Figure 18 – View from AR.Drone in flight
(not from the test)**

In Figure 17, the operator uses both cameras at the same time; the frontal view is centered while the bottom cameras view is in the upper left corner of the screen.

As mentioned, for a quadrotor used for military purposes it might be a good idea to have a GPS system combined with the live video operated system. The autonomous GPS system is used to fly the quadrotor to the area or object that is to be explored and then letting the operator take control over the quadrotor. It is even more important that the system that holds the quadrotor at the same position in hover is improved for this application since there most likely will be a delay before the operator sees the video depending on what link is used. The movements of the quadrotor would then have to be in small steps and continuously stopping and observing the surroundings, in these stops it is important that the quadrotor can hold its position to avoid drifting into the walls and crash.

4. Military benefits

In this chapter, an investigation of how the military could benefit from using quadrotors in their arsenal follows. Since current Swedish UAV policy states that no armament is allowed to be carried on UAV's the main military benefits are to be focused onto reconnaissance and transportation.

4.1 Short range supply

Soldiers that are on a mission behind enemy lines could by various reasons need resupplies in the form of ammunition and medical equipment for example. A quadrotor UAV could deliver such supplies behind enemy lines and get out safely when the soldiers are dangerous low on supplies. The soldiers will have to find a small open area and send their coordinates to the headquarters, the UAV will there be loaded with ammunition and medical supplies. When the UAV is loaded it will automatically take off and land on the specified coordinate using GPS. The unit behind enemy lines will then unload the UAV and press a button on it which makes it return to the main base automatically using another route to avoid detection. Different sizes of the UAV could be designed depending on the environment that the unit is fighting in. Smaller UAV's would be able to land in very small openings between the treetops while bigger UAV's will have to land on larger areas but carrying more supplies. Doing the resupply by night and when its foggy will reduce the risk of being spotted. Using electrical engines if possible will also reduce the risk.

4.2 Extended sight ("utflyttbart sikte"[in Swedish])



The idea here is to use a quadrotor UAV as a movable sight mounted on a ground vehicle, such a system could be used with benefit on a tank or other army vehicle to explore an urban environment without exposing the tank to a risk. The quadrotor is intended to be powered with a cable which also makes it a tethered configuration, this is important since it greatly simplifies the airworthiness certification of an eventual product since complicated Swedish UAV regulations don't apply for these kind of applications. Another positive benefit is that the signal from the quadrotor goes through an optical or galvanic cable which makes it hard for the enemy to detect the signals. This is the part of the report that most work is to be focused on since there might be an actual need for such a product in the near future. This part of the report focuses on the electrical systems powering such a configuration, direct current, alternating current, and the use of transformers to minimize the weight and the power loss in the system are to be discussed and analyzed. The information of this part of the report is to function as an initial feasibility analysis to assist in evaluating the potential of a possible future demonstrator of this concept.

4.2.1 The cable

Irrespectively of what power source one chooses to run the quadrotor on, one has to deliver the power from the source by a cable that needs to be highly flexible and light, it must also be able to carry the required power to the UAV without too high power losses and overheating. To get the cable as flexible and light as possible one should minimize the cables square section area. This is done by minimizing the current going through the cable, and that can be done by designing the UAV to run on a high voltage system. One can also minimize the weight of the cable by choosing a conductor that has a low conductivity to weight ratio, this is done by dividing different conductor's conductivities with their density, aluminum is found to be the best suited conductor for this application. The power loss in the cable can be expressed by following equation.

$$P_{loss} = \frac{\rho_r \cdot L}{A} \cdot I^2 \quad (9)$$

Where the term $\frac{\rho_r \cdot L}{A}$ corresponds to the resistance of the cable. The loss in the cable will result in a temperature increase and a loss of electrical potential in the cable. The temperature increase will result in a higher resistance in the cable and this has to be taken into account. It was first thought that the heat convection from a metallic cable was 5 W per square meter for every degree difference in temperature between the metallic and the air since this is a fair approximation for the cooling of different electronic systems. When the first calculations on the cables were made, it showed that the temperature would be the limiting factor when designing the cable. Therefore a test setup was made where one could drive a current through copper cables with different cross sectional areas. It was then found out that the heat convection unit was as high as 65 W · K/m² instead of 5 W · K/m² that was first assumed. The big difference between the first assumed value and the measured one is probably due to scale factors, comparable to Reynolds number. The used wires are much smaller than referenced dimensions. The value

obtained holds for aluminum cables as well since it is only the surface temperature of the metal that determines the convection of heat into the air. With this knowledge the temperature increase of the cable can be expressed by the following equation.

$$\Delta T = \frac{P_{loss}}{A_m \cdot Q} \quad (10)$$

Note that all temperature based calculations are done by assuming a room temperature of 20°C. Another aspect to take into account is that the strength of aluminum is reduced as the temperature increases; therefore one should be careful not to have temperatures much higher than 100-150°C. The resistance of the cable increases with this temperature increase and equation (11) shows how this is depending on the temperature.

$$\rho_r(T) = \rho_0 [1 + \alpha_0 (T_c - T_0)] \quad (11)$$

Where the temperature coefficient $\alpha_0 = 0.0039 \text{ K}^{-1}$ for aluminum at room temperature. Using these three equations in the order that they are presented within a loop in *MATLAB* (in order to reach an equilibrium temperature) one can calculate the temperature increase and the total resistance per meter cable. Using this information combined with Ohm's law and basic physics, the length, temperature, and the potential drop of the cable is easily calculated. Table 7 show how a change in the cross sectional cable area A_{cable} changes the potential drop ΔU , temperature increase ΔT and the total length of the cable. Some fixed values have been chosen in order to obtain the values presented in Table 7, these are that the maximum cable mass is 200 g and that the current going through the cable is 7 A, these values is chosen to obtain a cable suited for the AR.Drone.

$A_{cable} [\text{mm}^2]$	$\phi [\text{mm}]$	$\Delta U [\text{V}]$	$P_{loss} [\text{W}]$	$\Delta T [^\circ]$	<i>Length</i> [m]
0.15	0.43	1042	7293	165	247
0.25	0.56	279	1953	57	148
0.35	0.67	131	915	32	105
0.45	0.76	76	533	21	82
0.55	0.84	50	349	15	67
0.65	0.91	35	247	12	57
0.75	0.98	26	183	9	49
0.85	1.04	20	142	8	43
0.95	1.10	16	113	6	39

Table 7 – Aluminum cable properties vs. Cable cross sectional area

An aspect to keep in mind is that the cable temperatures will increase significantly if the cable is rolled onto a roller and that a cooling device might be needed. Some thought has also to be put into how the cable is to be isolated, if there is a fairly low potential difference between the cables some kind of lacquer might be sufficient to isolate the cables from each other, a thin isolator is preferred since these do not reduce the heat convection as much as thicker ones. A good idea to better understand how the cable needed for this application should look like might be to study the wire that is used to control wire guided missiles, since both applications are quite similar to each other. It is important to use a number of smaller wires to lead the current to the vehicle instead of just one wire. There are two reasons for this, the first is that using smaller wires will lead to a more flexible cable; the second is that it results in a smaller temperature increase of the cables. The reason for the temperature decrease is due to the fact that smaller wires have more mantle area per total cross sectional area compared to larger wires. This is the case as long as one does not combine the wires into one larger wire. The resistance of the cables does however grow when the cable cross sectional area is decreasing, but the total resistance is not changed since the current is split between the different cables. Worth to mention is that the potential drop in the cable also doesn't change when it is divided into a number of smaller ones but with the same total cross sectional area. Figure 19 shows how the temperature of the wires is decreasing when the number of wires is increased for an aluminum cable with a total cross sectional area of 0.15 mm^2 .

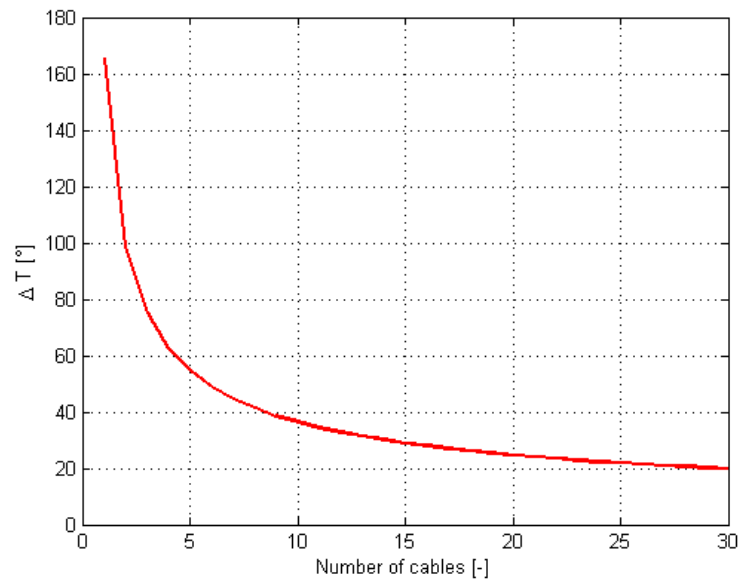


Figure 19 – Aluminum temperature decrease vs. Number of cables

A company called *Nexans* claims after talking to them that they produce aluminum cables but they do not sell them in small quantities. Since this work is to be used as an underlay for the build of a demonstrator, the work above is done for a copper cable as well since no suitable aluminum cables was found for sale.

$A_{cable} [mm^2]$	$\varnothing [mm]$	$\Delta U [V]$	$P_{loss} [W]$	$\Delta T [^\circ]$	$Length [m]$
0.15	0.43	159	1110	83	76
0.25	0.56	49	340	33	48
0.35	0.67	24	165	19	32
0.45	0.76	14	97	13	25
0.55	0.84	9	65	9	20
0.65	0.91	7	46	7	17
0.75	0.98	5	34	6	15
0.85	1.04	4	27	5	13
0.95	1.10	3	21	4	12

Table 8 – Copper cable properties vs. Cable cross sectional area

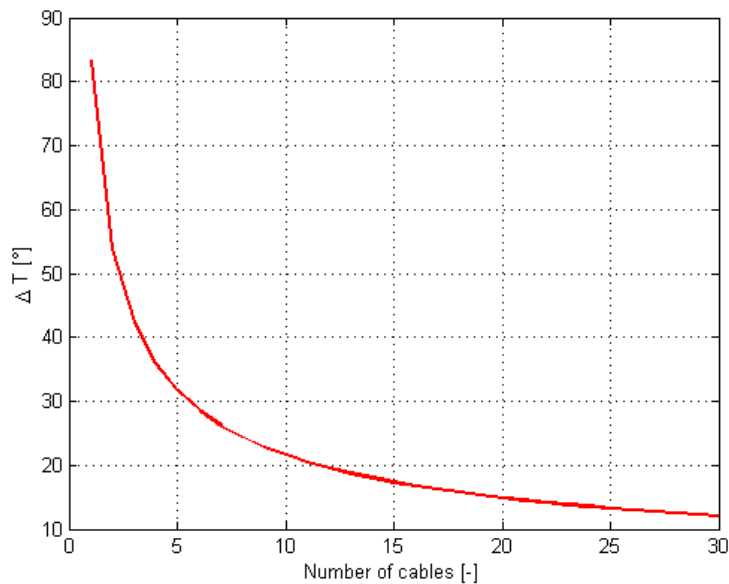


Figure 20 – Copper temperature decrease vs. Number of cables

4.2.2 DC-system

Swedish regulations states that potentials below 75 V require no specific electrical certification, this part of the report focuses on the performance of a quadrotor powered with a direct current source with a maximum potential of 75 V that is delivered to the quadrotor by a cable from the ground. There are a few ways to optimize this system, one way is to choose an optimal electric potential to run the quadrotor with, based on the power consumption required to maintain the quadrotor in hover, the following lines of text describes how to choose the optimal electrical potential with the goal to maximize the length of the cable.

If the maximum mass of the cable is known, the length of it can be calculated using equation (12).

$$L = \frac{m_{cable}}{A \cdot \rho_{metal}} \quad (12)$$

The electrical potential of this system is described by equation (13).

$$V_{source} = V_{cable} + V_{quad} \quad (13)$$

Where V_{source} , V_{cable} and V_{quad} is the potential over the battery, cable and the quadrotor. Using Ohm's law and inserting the expression for the length of the cable in equation (13) with the knowledge that the

resistance of a cable is described by $R_{cable} = \frac{\rho_r \cdot L}{A}$, one gets the following expression for the electrical potential of the system:

$$V_{source} = \frac{\rho_r \cdot m_{cable}}{A^2 \cdot \rho_{metal}} \cdot I + V_{quad}$$

Solving this equation for the cross sectional area in *MATLAB* for different currents under the condition that $V_{quad} = \frac{P_{quad}}{I}$ (the power needed to drive a quadrotor can be estimated, an explanation of how to do this is done in chapter 6 of the report) enables one to plot the obtained cable length as a function of the current. This is done for the known parameters of the AR.Drone and can be seen in Figure 21.

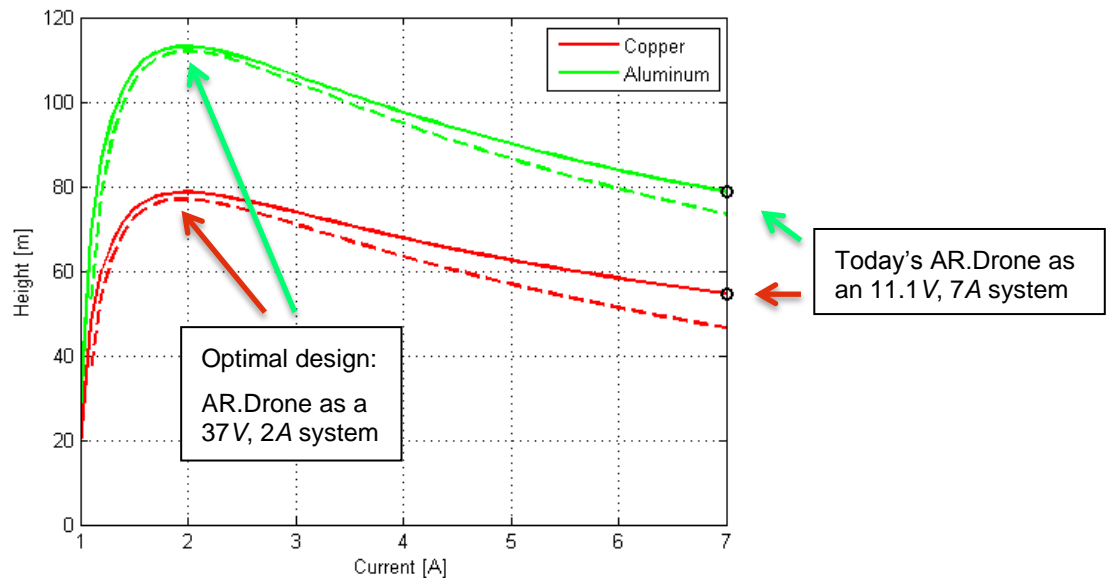


Figure 21 - Height vs. Current

The black circles in Figure 21 represent the height AR.Drone could reach as it is currently designed as an 11.1 V system. Designing the quadrotor to operate at 37 V instead would increase the height with approximately 40 % for both cables, since $V_{quad} = \frac{P_{quad}}{I} = \frac{74}{2} = 37$ V. It is therefore clearly important to design the quadrotors electrical system to operate at optimum potential in order to maximize the height of the system. The dotted line in the graph represents the actual height that is obtained due to the temperature losses stated in section 4.2.1.

Note that increasing the allowed mass of the cable with a factor of 2 increases the height with a factor of $\sqrt{2}$, and that the height described in Figure 21 is the length of the cable divided by two since this is the height that the quadrotor could reach with a cable that consists of two conductors.

4.2.3 Extended sight – Ground forces version

Swedish armed ground forces could get valuable information of their near surroundings if using a quadrotor equipped with various sensors. But it is important that the quadrotor do not reveal their position to the enemy, this means that the quadrotor most likely would be sent up in the air for short periods of time and that the information from the sensors would have to be transmitted by a cable to the ground. Another important factor is the sound signature of the quadrotor, brushless in running engines needs to use a gearwheel to connect the propeller from the engine; this gearing generates a lot of noise which could lead to detection. This could be prevented by choosing an outrunning brushless engine instead; these produce more torque, and this makes it possible to connect the propeller directly to the engine axis which eliminates the need for noisy gearwheels.

Since the time that the quadrotor needs to remain in hover to avoid detection is short, it is always better to use a battery instead of supplying the quadrotor with energy from the ground because there will always be significant losses in the cable. The loss in the cable for the optimal designed DC system is actually the same that is required to propel the quadrotor. This means that propelling the quadrotor from the ground would result in half total flying time for the quadrotor with a given amount of carried batteries. But there are however situations when the ground forces might need to have a quadrotor in the air for a larger amount of

time to keep lookout for the enemy in order to prevent them from being ambushed. In this case a quadrotor powered from the ground would be the best alternative.

4.2.4 Extended sight – Tank version

The tank version of this quadrotor was decided during a meeting with the *FMV* to have a maximum width and depth of 1.2 m, and weigh a maximum of 10 kg. The quadrotors sensor payload is set to 1 kg based on the previous work done in the Pegasus project. In order to make the quadrotor as efficient as possible, the largest possible rotor radius of 0.3 m is chosen. Based on the model described in chapter 6, but without the mass of batteries and added mass of the cable the required power to propel such a quadrotor is calculated. The efficiency of the platform is set to 0.33 since the quadrotors on the market reach these values. Using the same model to calculate the maximum length of the cable as in section 4.2.2 but with the exception that the maximum allowed mass of the cable can be varied, it is possible to plot the maximum height that can be achieved for different cable masses. The plotted height is the reduced height due to heating of the cable.

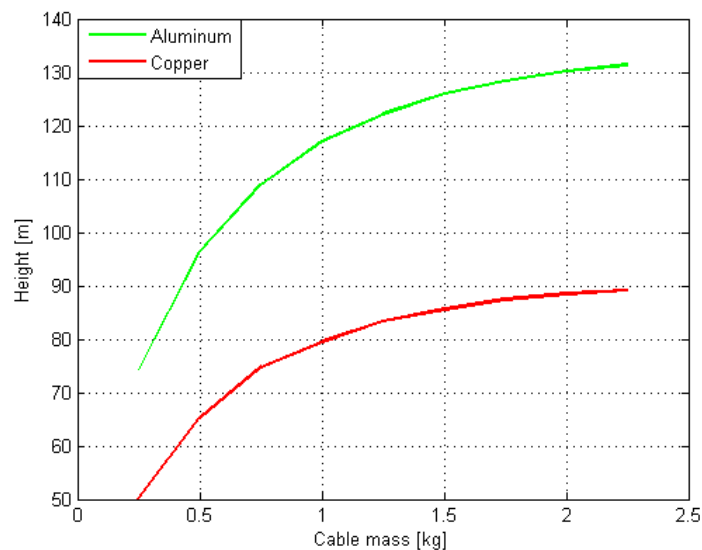


Figure 22 - Height vs. Mass of cable

Figure 22 shows that the height that is gained by adding cable mass is very conservative, this is the case since adding cable mass results in a more power consuming quadrotor which leads to more losses in the cable and a significant higher total power consumption of the system as a whole. Note that it is for a cable mass of 0.25 kg that one obtains most meter cable per watt spent. Using a 75 V power supply, makes it hard to reach a height higher than 130 m no matter of how much cable the quadrotor is allowed to carry. The only way to obtain higher heights is to make the quadrotor consume less power when in flight. This could be done by adding ducted fan propellers to the quadrotor instead of conventional ones.

4.2.5 High voltage systems

It is not possible to use a high voltage system due to safety regulations so no further analyzes is done under this subject except for stating that this is the most optimal choice since cable losses would be minimal using high voltage systems. One could use high voltage in the cable combined with transformers in the quadrotor to obtain the desired voltage. But transformers are quite heavy so the optimal solution would probably be to design the quadrotor so that its engines run on the high voltage and have a small transformer that generates the current required for the ESC (Electronic Speed Controller).

4.2.6 Aerodynamic forces acting on the cable

The wind blowing on the cable will result in an aerodynamic drag force that is ultimately affecting the quadrotor. For the case that the quadrotor carries a 1 kg aluminum cable, the length of it would then be 117 m (Figure 22) and its diameter is 1.4 mm, the quadrotors total weight including the cable would then be approximately 3.3 kg on the model described in chapter 6. The cable could be modeled as a long cylinder hanging freely in the air. The wind speed is set to 15 m/s and is purely horizontal. Equation (14) gives the Reynolds number for these values:

$$R_e = \frac{\rho v L}{\mu} = \frac{1.225 \cdot 15 \cdot 1.4 \cdot 10^{-3}}{1.8 \cdot 10^{-5}} = 1429 \quad (14)$$

Figure 23 shows a simplified model of what forces that are acting on the system.

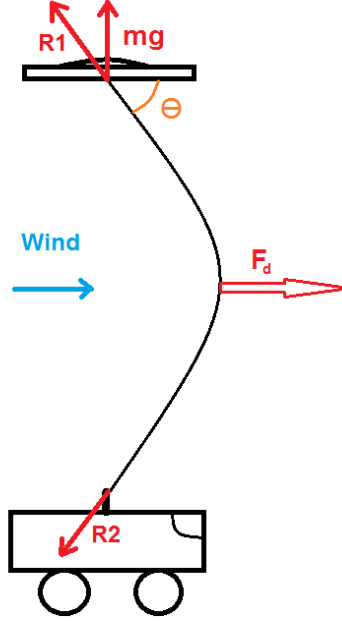


Figure 23 -Forces acting on the system

Hoerner is a German scientist that made a lot of work on aerodynamic drag and lift in the mid-20th century, he made some work on aerodynamic lift and drag acting on a cable holding a kite. This results in a drag force and lifting force acting on the cable. But since the quadrotor provides its own lift the cable is always hanging freely in the air down to the vehicle and the only force acting on the cable is therefore the drag force since the sum of all lifting force contributions is zero (positive lift is gained on the upper part of the cable while the same negative lifting force is acting on the bottom part of the cable). The drag coefficient C_d for a cylinder at a Reynolds number of 1429 is approximately 0.9. It is assumed that the cable is straight from the quadrotor to the mid-point where the force F_d is acting (even though is not drawn this way) with an angle theta. The force acting on the cable is described by equation (15):

$$F_d = \frac{1}{2} \rho V^2 C_d A_p \quad (15)$$

Where A_p is the projected area of the cylinder perpendicular to the wind.

$$A_p = 117 \cdot \sin(\theta) \cdot 1.4 \cdot 10^{-3} \quad (16)$$

Since a cable can only take forces along its direction, the forces that are acting on the quadrotor and on the vehicle are described by equation (17).

$$R_1 = R_2 = \frac{F_d}{2} \cdot \frac{1}{\cos(\theta)} \quad (17)$$

The total thrust that the quadrotor must generate under these conditions is then described by following equation based on vector normalization.

$$T_{tot} = \sqrt{(\cos(\theta) R_1 + mg)^2 + (\sin(\theta) R_1)^2} \quad (18)$$

Since the angle θ is hard to estimate the total thrust force is calculated for a couple of different possible values of this angle and presented in Table 9.

Θ	T_{tot}	T_{tot}/mg
85	123	3.81
80	71	2.19
70	49	1.52
60	44	1.36
50	41	1.27
40	39	1.21
30	43	1.33
20	37	1.16
10	34	1.05

Table 9 - Forces vs. Θ

One can see that for the case that the angle Θ is about 85° the quadrotor need to produce almost four times the thrust than it would have had to produce under wind free conditions. This means that if the quadrotor can't produce this amount of thrust it will lose altitude until the angle Θ has decreased enough that it is able to produce the required thrust.

4.2.7 Alternative to the quadrotor platform

There have been done some interesting work on different VTOL platforms during the 1950's; one of them is the Hiller helicopter which can be seen in Figure 24.

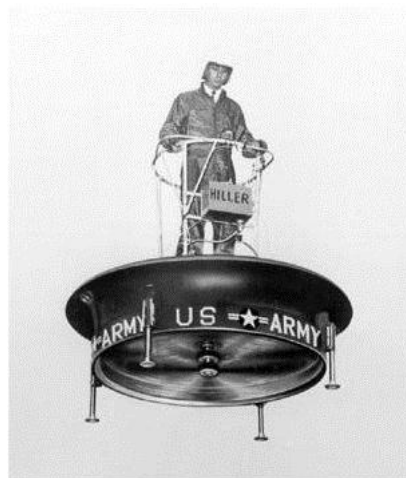


Figure 24 - Hiller helicopter

It consists of two counter rotating propellers in a ducted fan configuration. The use of counter rotating propellers gets rid of the moment created from the engines and the ducted fan configuration provides 50 % extra static lift. This aircraft was controlled by leaning in the direction the pilot wanted to fly (just like a bicycle) and with the aid of control vanes.

The proposal for the alternative to the quadrotor platform to be used as an extended sight builds on this principle. It could consist of two counter rotating propellers in a ducted fan configuration, this gives the advantage of a more simple and robust design that requires less engines. Either one engine or two engines can be used to propel this aircraft depending on how the counter rotating propeller is chosen to be driven.

The stability of this aircraft is obtained by using a moment wheel onboard the aircraft which resists attitude changes in all directions except for the axis it is spinning on. This axis should be the same axis as the propellers are spinning on; controlling this axis is instead done by changing the rpm of one of the two counter rotating propellers. The moment wheel can either be heavy and spin with a low rpm or be light and

spin with a high rpm to give the same amount of stability to the aircraft, the latter is obviously preferred. There are magnetic bearings that are practically totally frictionless; which makes one able to use incredible high rpm's on the moment wheel. This makes one able to construct a moment wheel for this application without adding a lot of extra mass to the aircraft. Using frictionless bearings means that none or very little power is spent on keeping the wheel spinning so practically no extra energy is spent on the stability control. The most positive advantage this aircraft gains from using a moment wheel for stabilization is that it provides a stable platform for the camera onboard. This might make it possible to use cameras that can zoom much and still obtain good pictures/videos.

The attitude control is intended to be controlled by tilting the moment wheel in different directions, tilting the moment wheel results in a counter moment on the vehicle which can be used to control the aircraft. Satellites use this technology since it eliminates the need to spend valuable fuel to provide the attitude control in space. They use moment wheels spinning at high rpm's on a controllable gimbal suspension, this technology could also be used to control this alternative to the quadrotor platform and the quadrotor platform if desired. If this idea is totally discarded by the reader he should however keep in mind that moment wheels is often integrated in camera equipment placed on unstable platforms such as UAV's to produce steady pictures and videos and could be used for that application instead.

4.2.8 Extended sight flight strategy

It would be very tempting for the enemy to just shoot down the extended sight aircraft when spotted, this risk could be reduced by letting the aircraft move in random directions when in danger. Figure 25 illustrates how this random movement might look like in two dimensions.

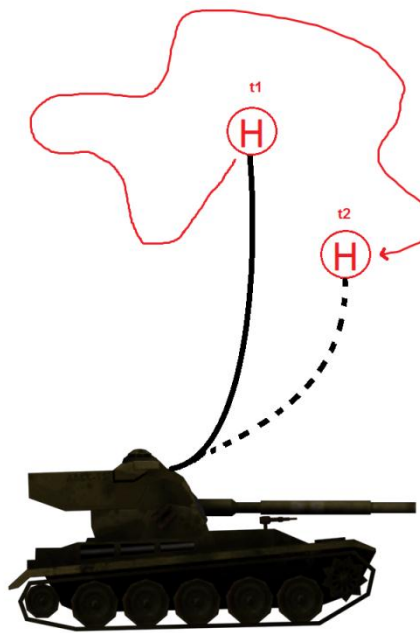


Figure 25 – Randomly moving extended sight

If it is assumed that the possibility of the aircraft being hit is 1 when hovering in the air. If one makes the aircraft move randomly in an imaginary cube above the vehicle the risk of it being hit is reduced significant. If the cubes sides are 10m each, then the risk of the quadrotor being hit is:

$$Risk = \frac{Volume_{quad}}{Volume_{cube}} = \frac{1.2 \cdot 1.2 \cdot 0.4}{10^3} = 0.0576 \%$$

The actual risk of the aircraft being hit is of course depending on more parameters such as which weapon is used to fire upon the aircraft and how fast the aircraft can move in this imaginary cube. But the calculated value gives a hint of the importance of implementing an evasive flight mode to the system. The aircraft should be able to do these evasive maneuvers autonomously and it might be possible to use some kind of sensor onboard that detects approaching bullets and starts the evasion mode automatically. The quality of the pictures and videos obtained from a camera placed on a moving platform would however suffer; this could be prevented by adding a moment wheel (gyroscope) to the onboard camera.

4.3 Flight strategies

Depending on what propulsive system one has chosen to propel the UAV, different flight strategies have to be analyzed. If the aircraft is propelled with an electric-hybrid system, a good idea could be to let the aircraft fly in a mode which leaves extra power to charge the batteries that can later be consumed at a more demanding flight. One could even land the aircraft and charge the batteries, and if the system is powered by sun cells this is probably the best way since there are very few aircraft that is capable of maintaining flight only on sun cells. There are even new kinds of infra-red sun cells that can charge the batteries even when the sun is covered by clouds. During a military mission, the mission time could be improved significant if one chooses to design the UAV for being able to land in enemy territory and do its surveillance from appropriate location which could be the enemy's roof top for example. From the roof the aircraft could carry out its surveillance using interception equipment and cameras or it could place out its surveillance equipment and fly to safety and charge its battery's.

5. Sizing effects

There are many important factors to take into account when one is trying to increase the size of a quadrotor helicopter, the performance of such aircraft is not proportional to the scaling multiplier. For airplanes however the Breguet range equation can be used quite satisfactory to calculate the range of an aircraft based on just how much fuel is burned. The lift to drag ratio roughly remains the same when resizing airplanes, but for a helicopter there is nothing like the Breguet range equation since there is no equivalence for the lift to drag ratio, this greatly complicates the calculation of range and the sizing of the helicopter to a range requirement. An investigation of how the different components of the quadcopter behave when they are increased in size is done in following chapter.

5.1 Square-cube law

When an object is proportionally increased in size, its mass and volume increases with the cube of the multiplier and its surface area is increased by the square. Another important aspect when increasing the size of an object is that it must be built more rigid if it is to be operating under the same conditions such as acceleration and speed, which is a direct consequence of the square-cube law.

5.2 Engines

The most electric motors available for RC-aircraft can comfortably run on a power output of 4.2 W/g without overheating, regardless of their size. A series of Hacker brushless RC-engines with different power outputs and weights has been used to confirm that power to weight ratio. This means that the increase in weight and power is completely linear. The efficiency of electric engines tends however to grow with their power output and therefore also their size. This can partly be explained by that larger engines have cables with higher cross-sectional area inside the engine which have less resistance. The most common electrical engines used for propelling UAVs are, brushless outrunning, brushed and brushless in-runner motors. Brushed engines are less effective than brushless due to the contact friction of the commutators and their only real advantage is that they are cheap and do not require an ESC. Brushless outrunning engines produce more torque than brushless in-running engines but are slightly less efficient, both engine types can reach an efficiency of larger than 90 %. The higher torque produced by these engines makes them popular to use when one is to choose a direct-drive propeller setup, while brushless in-running engines often requires a geared propeller setup. Another reason to choose brushless engines instead of brushed is that no rpm sensor is needed since this data can be got from the electronic speed controller required to control the brushless engine.

5.3 Rotor size

If one is keeping the thrust required to be produced from the rotor to a constant value, equation (3) shows that the power required to produce the same thrust is only depending on the total area swept out from the rotor. Figure 26 shows how the scaling factor of the rotor affects the ideal power required for one rotor to maintain the AR.Drone in hover, taking the weight increase of the propeller into account based on the square-cube law and implementing this weight increase in equation (3) by changing $T_h^{3/2}$ to $(m_p + T_h)^{3/2}$ where m_p is the mass of the propeller.

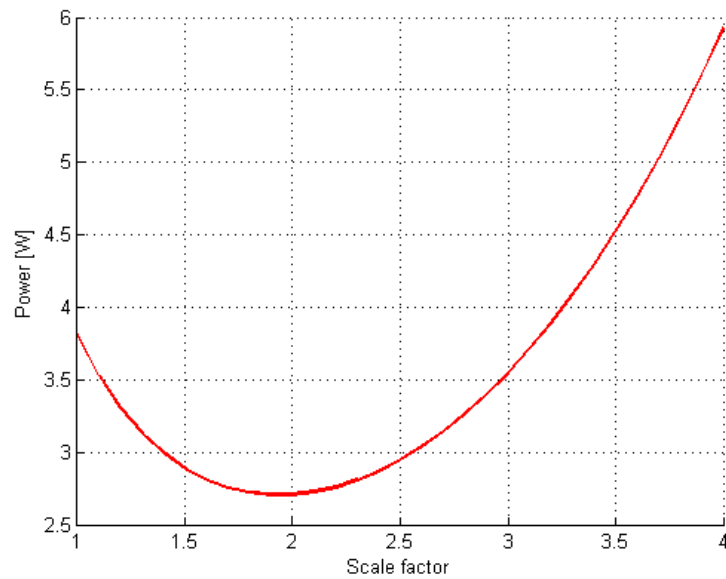


Figure 26 - Power vs. rotor size

Figure 26 shows that increasing the propeller size of the AR.Drone by a factor of two would require about half the power to maintain the same thrust. But increasing propeller size will also increase the overall size of the quadrotor which will result in a heavier aircraft so this is always a tradeoff. An attempt to verify how well the square-cube law works on propellers was done by taking data from the propeller manufacturer APC and using their smallest propeller as a reference, Figure 27 shows how these data fit according to the square-cube law.

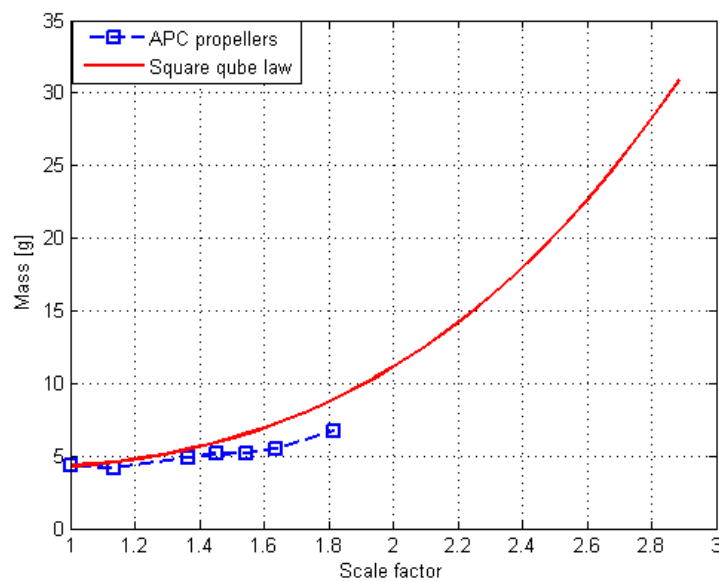


Figure 27 – Square-cube law & APC propellers

5.4 Agility with scaling

An agile quadrotor might be of interest when designing the extended sight quadrotor that has to be able to do agile evasive maneuvers in order to avoid being shot down. Small objects tend to be more agile compared to bigger ones; this is mostly due to the fact that the moment of inertia is proportional to the change in size of the object to the power of five. The next lines of text are dedicated to prove this. The moment of inertia of a point mass of 1 kg placed on a rod (assumed to be weightless) at a distance of 1 m from its axis of revolution is calculated using equation (19).

$$I_{1:1} = mr^2 = 1 * 1^2 = 1 \text{ kg} \cdot \text{m}^2 \quad (19)$$

If the point mass system is decreased in size by a factor of two, then the weight of the system has decreased with a factor of 8 (square-cube law), and the distance from its axis of revolution has decreased with a factor of two. The new moment of inertia of the system is then:

$$I_{1:2} = mr^2 = 0.125 * 0.5^2 = 0.0313 \text{ kg} \cdot \text{m}^2$$

This is exactly the same as putting the factor that the object is decreased in size to the power of five.

$$\left(\frac{1}{2}\right)^5 = 0.0313$$

6. Flight time approximation model

This chapter of the report is about simulating the maximum time a quadrotor of a given size and weight can maintain hover. These simulations are done in *MATLAB* and are built on the equation for the power required to maintain hover derived in chapter two.

$$P_h = \frac{T_h^{3/2}}{\sqrt{2\rho S}}$$

The information obtained from the reverse engineering of *parrots* AR.Drone quadcopter and by gathering known information from manufacturers of RC-parts such as batteries and engines is used to give a more precise approximation of the time in hover that one could be able to obtain. The model calculates the time in hover by knowing the total energy in the battery and the power consumption. The model also have a limit of the maximum allowed rotor disc loading to prevent the flight time curves to continue in infinity. This limit is set to four times the disc loading of AR.Drone in hover.

6.1 Mass model

It is commonly understood by aerospace engineers that the hardest part to get right of the design of an aircraft is to predict the weight of it. This chapter describes the mass model that is used to approximate the flight time of the quadrotor.

6.1.1 Propeller mass

The propellers mass was first approximated by using the square-cube law discussed previously in the report. The density of the COTS quadrotors propellers is assumed to be 1.2 g/cm^3 since this is a common value for plastic propellers. The propeller of the AR.Drone weighs 4 g, knowing this weight one can calculate that the volume of the propeller is 3.333 cm^3 . This volume is then used as a reference volume for a propeller with a rotor radius of 10 cm and the volume of all other propeller sizes is calculated by using this volume as a reference and the square-cube law. The mass of the next propeller in size is then calculated but with the exception that the material in the propeller is changed to carbon fiber reinforced nylon with the material density of 1.33 g/cm^3 to make it more robust. The mass of any propeller size is now described by following equation (20).

$$m_p = v \cdot \left(\frac{r_p}{r_{p,ref}} \right)^3 \cdot \rho \quad (20)$$

Where v is the reference propellers volume, ρ is the propeller material density, $r_{p,ref}$ is the reference propellers radius and r_p is the radius of the propeller which the mass is to be calculated for,

6.1.2 Engine mass

The power to weight ratio of a brushless electrical engine used in RC-aircrafts is approximately 4.2 W/g . This value is found out by investigating the power to weight ratio for engines on the market. Relating the ideal power required maintaining the AR.Drone in hover to the actual engine power capacity of the quadrotor; one can calculate that they have chosen an engine that is 4.77 times more powerful. This factor will be used in the model to calculating the mass of the engines. The mass of the engine controller board is about 0.03 grams per watt power output from the engine; this value is based on recommendations from the engine manufacturer *Hacker*. The formula for the mass of one engine in grams is therefore:

$$m_e = 4.77 \cdot P_h \left(\frac{1}{4.2} + 0.03 \right) \quad (21)$$

6.1.3 Structure mass

The structure mass of the quadrotor is calculated by knowing the propeller radius and the total weight of the known parts of the system. Carbon fiber tubes are used to construct the structure since these provide a light and strong structure that can resist large bending moments. Carbon tube structures don't however resist large forces in their axial direction so the structure was designed to resist 10 times its own weight in bending moment (each of the four quadrotors rods where designed to resist this load). The maximum allowed tensile stress for carbon fiber tubes is 600 MPa, and the density of these tubes is about 1800 kg/m^3 . The length of each rod is assumed to be 1.5 times the length of the propeller radius and the total weight of the quadrotor is assumed to be at the beginning of the rod. The bending resistance of a tube is described by equation (22).

$$W_b = \pi \cdot r_t^2 \cdot t \quad (22)$$

Where the thickness t is assumed to be $\frac{r_t}{10}$, since this is a common wall thickness of carbon fiber tubes. The bending stress is calculated by equation (23):

$$\sigma_{max} = \frac{M_b}{W_b} \quad (23)$$

Solving equation (23) for the required radius r_t makes it possible to calculate the mass of each of the four rods. Using the same tube thickness, one can construct a simplified version of the quadrotors structure that is as a function of the propeller radius only, Figure 28 shows how this structure looks like.

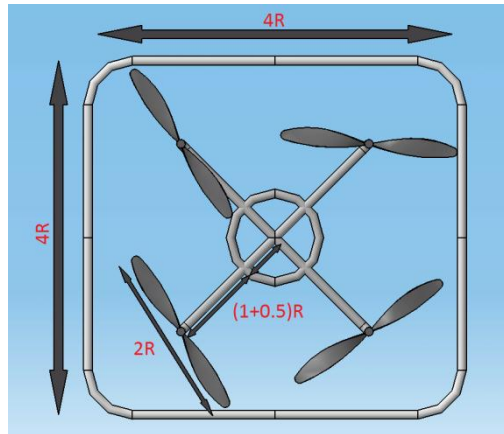


Figure 28 – Structure design

The necessary tube thickness is used everywhere to build the structure for simplicity, and the somewhat unnecessary outer protection ring is there to put some extra unpredicted weight on the structure. The inner circle is a rough approximation of the quadrotors inner body. The whole body has been designed to withstand significant larger forces than what is needed just in order to not be too lightly modeled since extra unpredicted weights are most likely to be present.

6.1.4 Miscellaneous mass

The weight of the mainboard of the AR.Drone is 22 grams, the misc. mass constant is set to be the twice of this value to account for the weight of cables and other electronics.

6.2 Efficiency

Since *Airspeed Industry's* test of the efficiency of the quadrotors propulsion system couldn't give the individual values of the efficiency for the engine and propeller and no time is left on the project to further investigate the efficiency curves for engines and propellers depending on their size, the efficiency in the flight time simulation model must unfortunately be set to a constant. The value of the efficiency is set to be 33 %; this value is based on calculations for quadrotors on the market and on the test that was performed by *Airspeed Industry*.

6.3 Energy density

Since this model is intended to simulate the flight time for both battery and combustion based systems, one has to take into account how the energy density varies with the weight of the system.

6.3.1 Li-Po

Lithium polymer batteries is the battery with the highest energy density on the market, this type of batteries has made it possible for electrically powered RC aircraft and helicopters to become as popular as they recently has become. Lithium polymer batteries have a theoretical cellular maximum energy density of about 200 Wh/kg, but it is not possible to reach this energy density on battery level where it matters. A study has been done on Li-Po batteries currently available on the market, the energy density of batteries from different producers have been calculated and from this study one can draw the conclusion that the specific

energy density varies from 140 to 148.2 Wh/kg depending on the weight of the battery if they weigh more than 57 g. The energy density grows slightly with the weight of the battery since it is harder to make smaller batteries with the same energy density as larger ones. Equation (24) describes how the energy density depends on the mass of the battery.

$$E_d = 142 + 7.6 \cdot m_b \quad (24)$$

There is however a restriction in the model that limits the energy density to rise above 148.2 Wh/kg since this was the highest energy density found on batteries available on the RC market.

Following figures show for how long a quadrotor of a given rotor radius and weight can hover with different payloads. These flight times has been plotted by using the equations stated in this chapter and then letting the battery mass vary for each fixed propeller radius. The different colored curves represent the flight time for each fixed rotor radius.

An example of how to read the graphs: The orange curve represents a rotor radius of 0.4 m; this can be seen by looking at the color bar to the right of the graph where orange represents a value of 0.4. The orange curve peaks at a mass of 6.6 kg and have a value of 43 min at this point. This means that a quadrotor that weighs 6.6 kg that have a rotor radius of 0.4 m can fly for 43 min using Li-Po batteries. The orange curve cross the x-axis at 2, this means that the dry weight of the quadrotor is 2 kg when no batteries are carried.

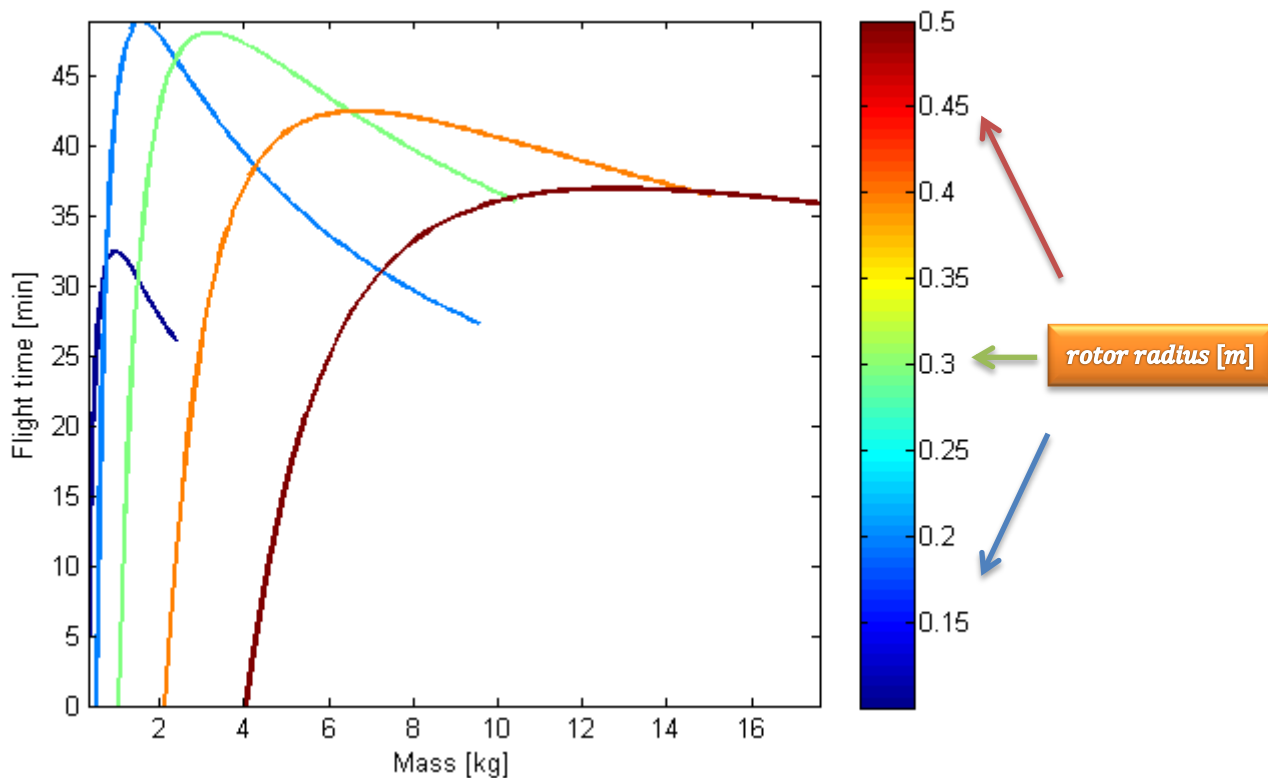


Figure 29 - Flight times with 0.2 kg payload

Figure 29 shows that the maximum flight time of 49 minutes is obtained by designing a quadrotor that has a rotor radius of 0.2 m that weighs 1.56 kg. Some important data for this particular quadrotor is presented in the tables underneath.

Total mass [kg]	Battery mass [kg]	Structure mass [kg]	Propellers mass [kg]	Payload [kg]	Engines mass [kg]	Misc. masses [kg]
1.56	0.9	0.215	0.142	0.2	0.051	0.044

Table 10 - Weight data for the optimal quadrotor that is carrying a payload of 0.2 kg

Engine power (each) [W]	System Efficiency [%]	Propeller radius [m]	Flight time [min]
65	33	0.2	49

Table 11 - Other important data for the optimal quadrotor that is carrying a payload of 0.2 kg

Figure 30 shows the flight times for different quadrotors that are carrying a payload of 0.5 kg.

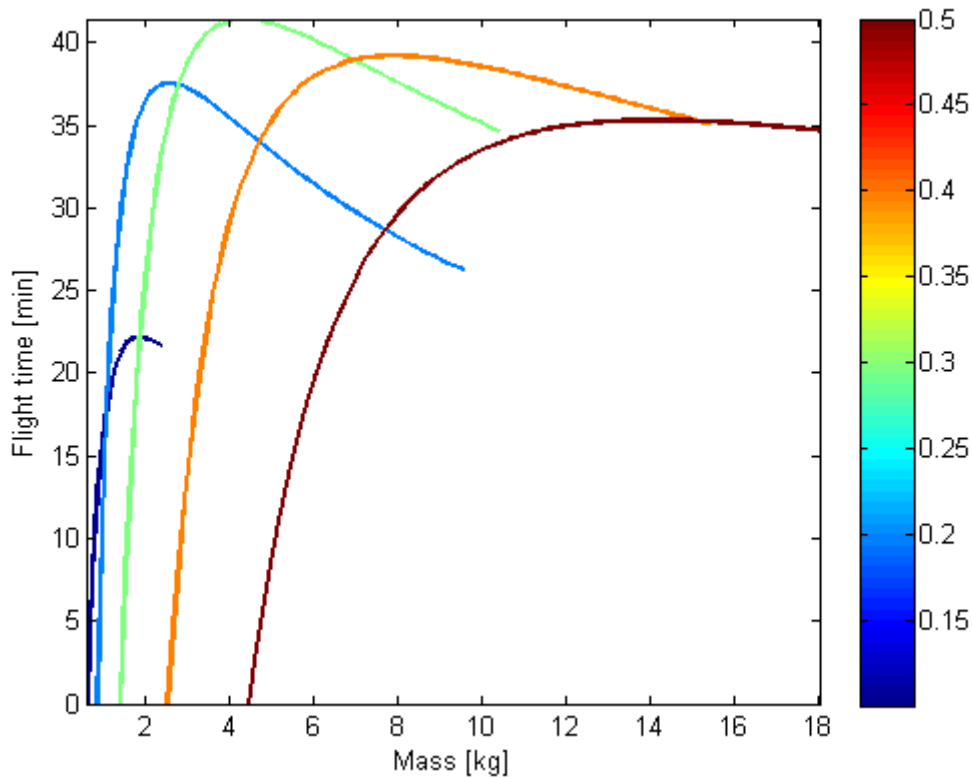


Figure 30 - Flight times with 0.5 kg payload

The optimal flight time of 42 min is obtained for a quadrotor with a rotor radius of 0.3 m. The data for the quadrotor is presented below.

Total mass [kg]	Battery mass [kg]	Structure mass [kg]	Propellers mass [kg]	Payload [kg]	Engines mass [kg]	Misc. masses [kg]
4.26	2.3	0.794	0.480	0.5	0.143	0.044

Table 12 - Weight data for the optimal quadrotor that is carrying a payload of 0.5 kg

Engine power (each) [W]	System Efficiency [%]	Propeller radius [m]	Flight time [min]
194	33	0.3	42

Table 13 - Other important data for the optimal quadrotor that is carrying a payload of 0.5 kg

Figure 31 shows the flight times for different quadrotors carrying a payload of 1 kg.

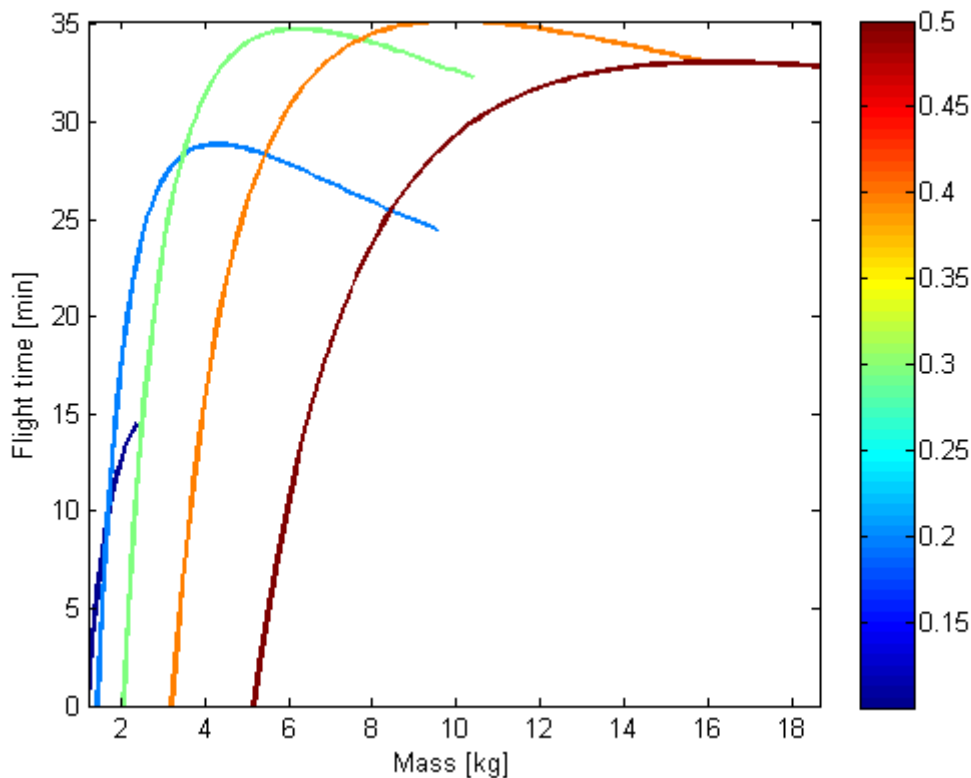


Figure 31 - Flight times with 1 kg payload

For this payload the optimal quadrotor radius is 0.4 m and has a maximum flight time of 36 min. But if one is decreasing the rotor to 0.3 m the flight time is 35 min instead of 36 and weighs 3 kg less, for these reasons this is chosen to be the optimal quadrotor instead of the one with the 0.4 m rotor radius. The data for this quadrotor is presented in the tables below.

Total mass [kg]	Battery mass [kg]	Structure mass [kg]	Propellers mass [kg]	Payload [kg]	Engines mass [kg]	Misc. masses [kg]
5.98	3.2	1.009	0.480	1	0.242	0.044

Table 14 - Weight data for the optimal quadrotor that is carrying a payload of 1 kg

Engine power (each) [W]	System Efficiency [%]	Propeller radius [m]	Flight time [min]
322	33	0.3	35

Table 15 - Other important data for the optimal quadrotor that is carrying a payload of 1 kg

An important aspect that is valid for all graphs is that one should be careful of defining what is the optimal quadrotor, in the case for the quadrotor above with a rotor radius of 0.3 m carrying a payload of 1 kg, decreasing the battery weight with 1 kg would only result in a reduction in flight time of 1 min. The graphs are constructed in a way that necessary structure and engine masses are calculated for varying battery masses. These masses do not vary very much with small changes of the battery mass. This means that by looking in the graphs and reducing 1 kg of the quadrotors total mass is almost equivalent of removing 1 kg of battery.

Another interesting phenomenon is that all graphs are showing that at some point the performance will stop to increase no matter of how big you make the quadrotor; the graphs also show that optimal rotor radius is depending on the payload that is being carried. One reason for that the performance starts to decrease at some point is that the batteries has the same weight during the whole flight while fuel based systems lose

weight at the rate that fuel is burnt. This means that battery based quadrotors are limited in how big they can be made.

6.3.1.1 Conclusion

Battery based quadrotors are limited in their size and endurance since making them too big for a given application would just result in a reduction of performance. This finding is a bit controversial for aerospace engineers since they are usually used to that increasing the size of an airplane will improve the endurance of it.

The endurance of a quadrotor is depending strongly on its weight and on the rotors radius, where the weight is the dominating factor of these two. There are three main parameters that the endurance of a quadrotor depends on; these are the rotor radius and the mass of the batteries and payload. These are the parameters that the designer can choose to change in order to obtain longer endurance.

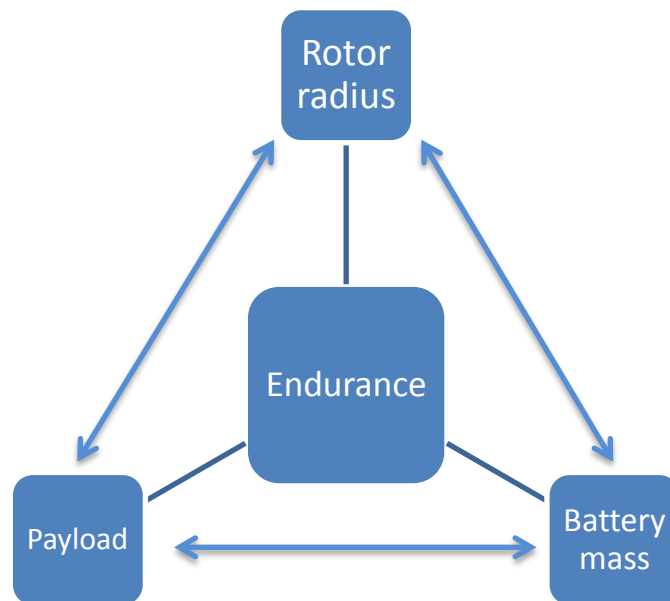


Figure 32 - Parameters that affect the endurance of a quadrotor

A short example of how to optimize the endurance of a quadrotor is to be followed:

Example: FMV wants to construct a quadrotor that should be able to hover with a 500 g payload for as long time as possible. The payload is now fixed, the parameters one can choose to change is the mass of battery and the rotor radius. A big rotor radius is always decreasing the power consumption of the quadrotor, but since the weight of the quadrotor is increasing with higher rotor radius, there will therefore be an optimal rotor radius for any given payload. The idea here is to use *MATLAB* or equivalent program to plot the endurance while varying these parameters. The endurance curves presented in this report is done by fixing a rotor radius and varying the mass of the battery, repeating this procedure for different rotor radius. Each of these curves is saved and plotted in the same graph and the best performing quadrotor is then chosen.

6.3.1.2 Micro is the future

This part of the report focuses on how the future of battery based quadrotor might look. The flight times for small quadrotors are calculated and show an interesting phenomenon that the time in hover actually increases significantly. Before this is done there are a few assumptions that have to be made. The first one is that components can be made as efficient as for the larger ones (33% efficiency). The second is that the payload consists of some kind of micro video sensor and that it combined with the ESC do not weigh more than 2 g. Figure 33 shows the predicted flight times for these micro quadrotors.

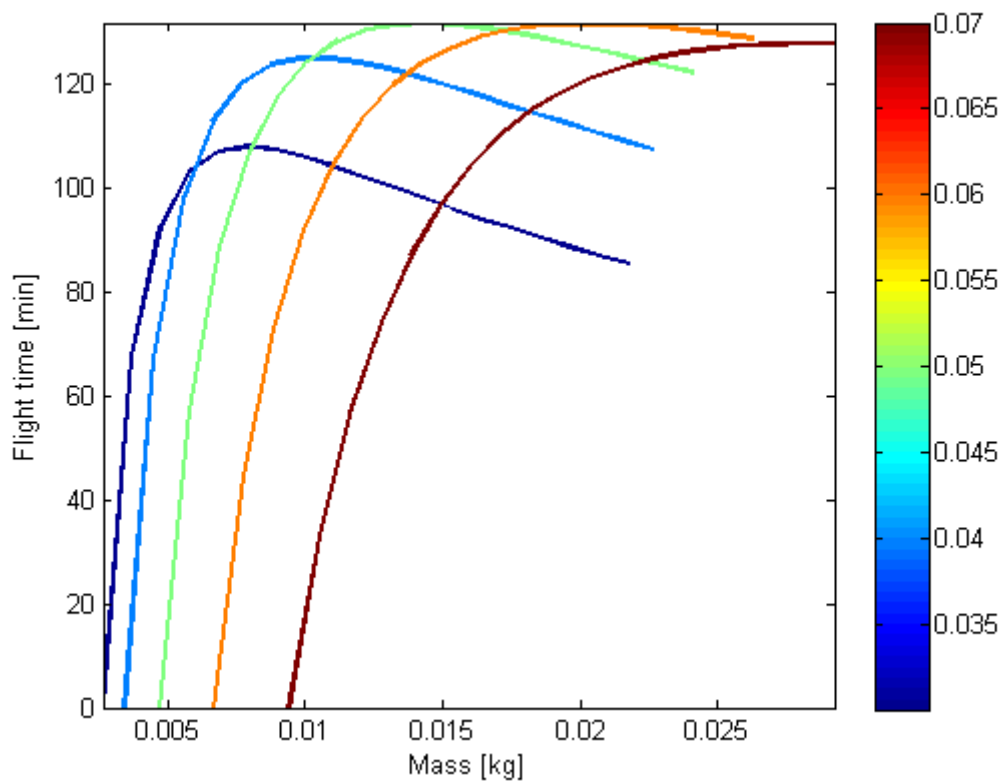


Figure 33 - Flight times for micro quadrotors

Figure 33 shows that flight times of over 131 min could be reached building micro quadrotors. Tables below show the data for the best performing quadrotor.

Total mass [g]	Battery mass [g]	Structure mass [g]	Propellers mass [g]	Payload [g]	Engines mass [g]	Misc. masses [g]
13.4	8	0.94	2.22	1	0.19	1

Table 16 - Weight data for the optimal micro quadrotor

Engine power (each) [W]	System Efficiency [%]	Propeller radius [cm]	Flight time [min]
0.18	33	5	131

Table 17 - Other important data for the optimal micro quadrotor

The quadrotors flight time would be 125 min if the battery mass is decreased with 3 g, if this weight is added to the components of the quadrotor instead it might be impossible to construct such a quadrotor with today's technology. The reason for this big improvement lay within the equation (3). The power required is depending on the weight of the quadrotor and the rotor radius.

$$P \propto \frac{T_h^{\frac{3}{2}}}{\sqrt{A}} \propto \frac{W^{\frac{3}{2}}}{r_p}$$

A simple example is followed of how this relates to the flight time. A given quadrotor weighs 1 kg and has a rotor radius of 0.2 m. The power consumption is then:

$$P_h = \frac{T_h^{3/2}}{\sqrt{2QS}} = \frac{1^{3/2}}{\sqrt{2 \cdot 1.225 \cdot 0.2^2 \cdot \pi}} = 1.3844 \text{ W}$$

If we decrease the size of the quadrotor with a factor of two, the weight would decrease according the square-cube law and the rotor radius would be the half, the power consumption is then:

$$P_h = \frac{T_h^{3/2}}{\sqrt{2\rho S}} = \frac{(1/8)^{3/2}}{\sqrt{2 \cdot 1.225 \cdot 0.1^2 \cdot \pi}} = 0.1224 \text{ W}$$

But the battery has also decreased its capacity with a factor of 8. If the large quadrotor have a battery that is capable of delivering 1.3844 Wh it would be able to fly for 1 h. Now we look at the time that the smaller quadrotor can fly, it now has a battery that is capable of delivering 1/8 of the original capacity. So the time that it can remain in hover is now:

$$\text{Time} = \frac{1.3844/8}{0.1224} = 1.41 \text{ h}$$

This means that the time that the smaller quadrotor can maintain itself in hover has increased with 41 %.

6.3.1.3 Validity of the model

In order to validate the model created for the flight time model using Li-Po batteries, a quadrotor on the market is analyzed and its flight time is compared to the predicted flight time generated by the model. The quadrotor used to validate the model is *Microdrones md4-1000*, it has a rotor radius of 0.35 m, weighs 3.1 kg and carries a payload of 500 g. With this rotor radius and payload following graph is plotted by the model.

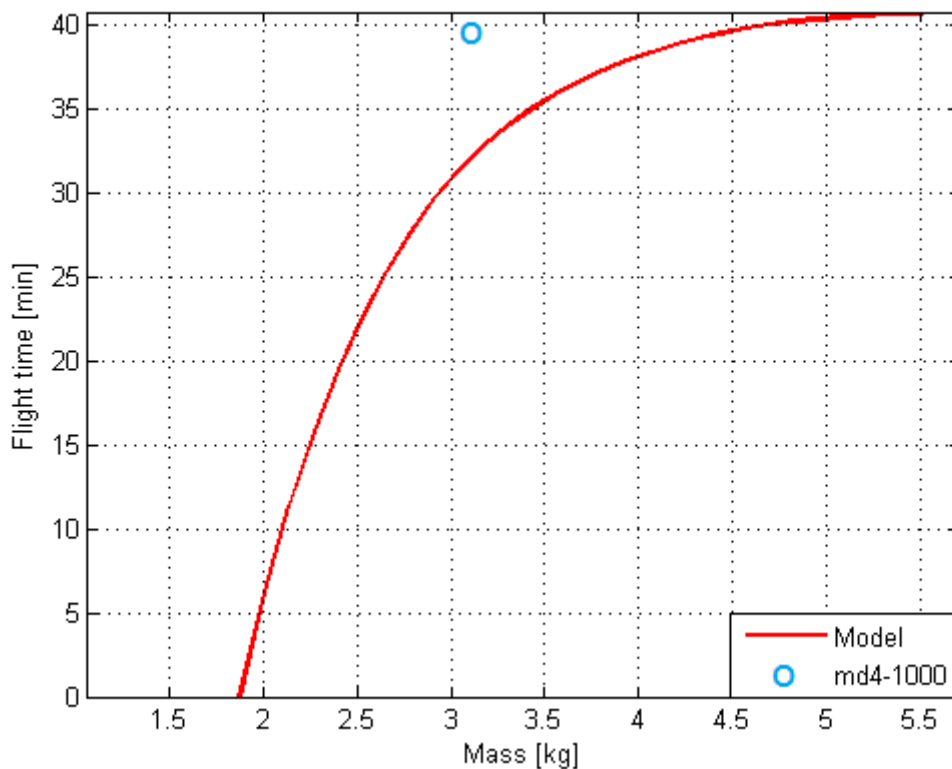


Figure 34 - Time approximation model vs. Reality

The blue circle in Figure 34 represent the actual stated flight time of the quadrotor carrying a payload of 500 g. The difference between the actual flight time and the approximated one is 6.5 min; this represents a deviation of 20 % between actual flying time and the predicted one. This moderate error could be reduced further if the efficiency could be implemented in the model. *Microdrones md4-1000* have an efficiency of 36 %, this is calculated from knowing the weight of the quadrotor, corresponding flight time and that its electrical system draws a current of 5 A on the ground. If this efficiency value is inserted in the model instead of its standard 33 % following graph is plotted:

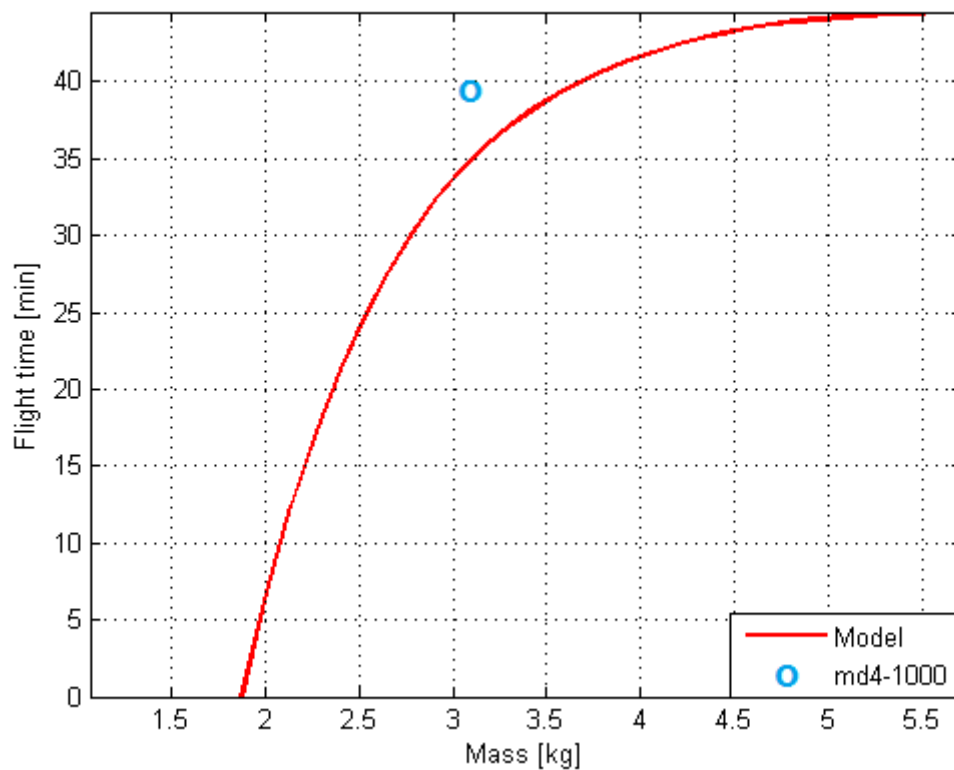


Figure 35 - Time approximation model (36 %) vs. Reality

Figure 35 show that the difference in time has now decreased to 3.5 min; which represents an error of 10%.

6.3.2 Hybrid system

Based on the previous work done in the Pegasus project, the energy and weight data from the suggested hybrid system is taken and implemented in this model and the maximum flight time is calculated. The chosen hybrid system is based on an 1154 W fuel engine used for RC-aircraft that uses a generator that converts all of the mechanical energy into electrical energy with a conversion efficiency of 52 % [3].

There are however some slight modifications to the model that has to be done in order to make it work.

1. The dry mass of the hybrid system is added into the mass model and the batteries mass is removed.
2. Fuel is added as a new power source, and its mass is added to the mass model but with the exception that the total fuel mass is continuously reduced as the fuel is burnt.
3. The fuel energy density is 12333 Wh/kg, the RC engines efficiency is 15 % and the generators efficiency is 52 %. This means that for every kg of fuel spent the quadrotor is able to consume: $P_{fuel} = 12333 \cdot 0.15 \cdot 0.52 \cdot 3600 = 3.46 \cdot 10^6 \text{ W}$
4. The last modification to the model is to limit the maximum power consumption to 1154 W since this is the engines maximum power output.

Since this engine is somewhat underpowered for this application only a few flight times can be calculated for a specific size of the quadrotor and no graphs is therefore presented as in the Li-Po section of the report. The performance is presented in the table below for the best performing quadrotor for a given payload and fuel capacity.

Payload [kg]	Hover time [min]	Quadrotor take off mass [kg]	Prop radius [m]	Fuel capacity [l]
0.2	233	6.9	0.3	4.3
0.5	213	7.3	0.3	4.3
1	138	6.7	0.3	2.9
1.25	129	7.0	0.3	2.9
1.5	121	7.3	0.3	2.9
1.75	113	9.1	0.4	2.9
2.5	53	7.3	0.3	1.4

Table 18 - Flight time vs. payload and fuel capacity

Even though the quadrotors engine is somewhat underpowered and the payload is small, an investigation of how long the quadrotor can travel and its total flying time is done, either if it is a reconnaissance mission or a mission to resupply soldiers. Three of the quadrotors stated in Table 18 weighs 7.3 kg and have a rotor radius of 0.3 m, the induced power of a quadrotor depend only on these factors. For all three quadrotors the following graph of the power required is produced:

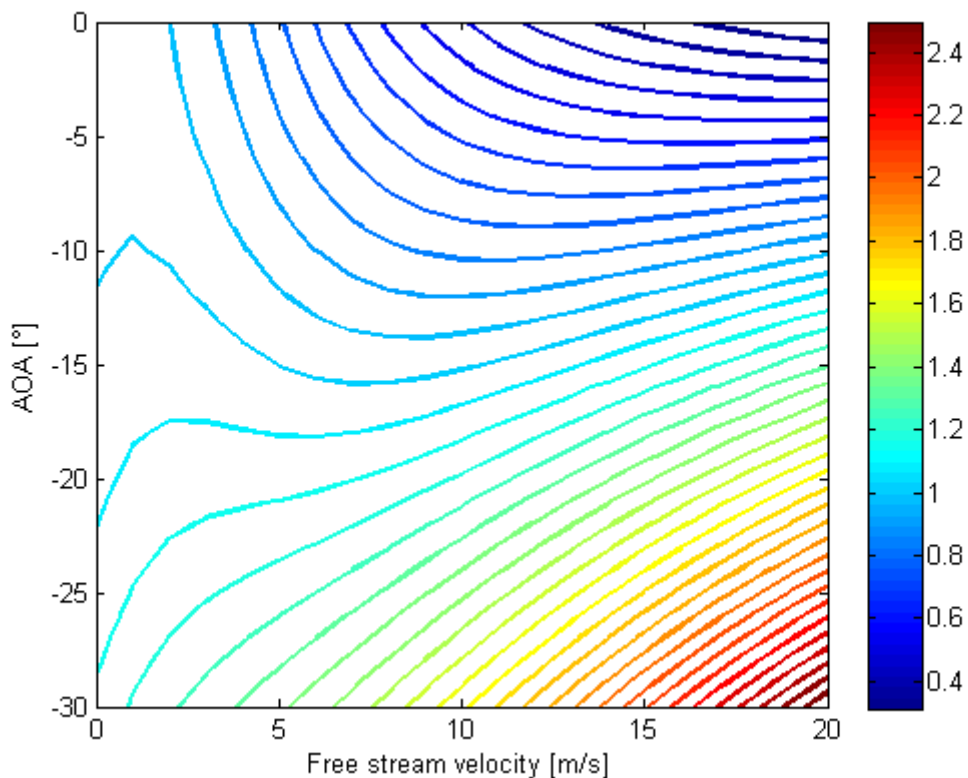


Figure 36 – Power required for a 7.3 kg quadrotor with a rotor radius of 0.3 m in horizontal flight

It is hard to predict exactly at what angle of attack the quadrotor will fly on, but it should be able to reach a speed of at least 20 m/s since *Microdrones* md4-1000 reach speeds up to 15 m/s. The induced power depends on the quadrotors speed and its angle of attack, and one could always choose a speed between 0 and 20 m/s where the angle of attack is low enough to give a significant increase due to the induced power effect. A value of 0.7 (which means that only 70 % of the power is used to fly the quadrotor) could be reached if the quadrotor is flying at a speed between 10 to 20 m/s with an angle of attack of -7° , which seems possible.

If we look at the quadrotor that is able to fly for 121 *min* with a payload of 1.5 *kg*, and assume that 5 *min* of its total flying time is spent on hovering on takeoff and landing and rest is spent on translational flight where the quadrotor benefits from the induced power. The endurance is then:

$$Endurance = 5 + \frac{(121 - 5)}{0.7} = 171 \text{ min}$$

If it is assumed that the quadrotor can fly at a speed of 15 *m/s* the maximum distance it could travel would then be:

$$Distance = (171 - 5) \cdot 15 \cdot \frac{60}{1000} = 150 \text{ km}$$

6.3.2.1 MW-8R

Another interesting idea, by the present author, is to increase the performance of a hybrid quadrotor by directly drive the propellers with the power from the engine to obtain more efficiency. Since the mechanical to electrical conversion efficiency is 52 % for such a system, if one chose to drive the propellers directly instead this loss could be greatly reduced. The aircraft should look something like the DraganFlyer X8, [9], which can be seen in Figure 37, it has two propellers on each of its four rods and the idea is to drive at least 80 % of the required lift to hover directly by the engine on the upper propellers and leave 20 % or less for the lower ones which are electrically powered in order to balance the system using the onboard ESC. The lower propellers are intended to be smaller than the bigger ones since they only need to produce a fraction of the total lift. Making the lower propellers smaller would also reduce the weight of the system and reduce the probable energy loss due to the propellers interacting with each other.



Figure 37 - DraganFlyer X8

The engine of this aircraft is placed in the middle and drives a gearwheel there, the four rods holding the propellers of the aircraft is made hollow and each of the hollow rods contains a shaft that is driven by the gearwheel in the middle, this shafts other end is connected to another gearwheel which drives the upper propellers. It should be possible to make this aircraft as light as the system that converts all of its mechanical energy to electrical energy since only 20 % of the power needs to be converted. This means that the battery and generators can be made much smaller, these components combined weighs 1.225 *kg* which is more than the engine weighs. This extra weight is intended to be used for the four extra smaller lower propellers and the drivetrain system. Another good aspect of this design is that the hollow rod and its inner shaft are somewhat already necessary structural features of the aircraft.

The drivetrain contains 8 gearwheels in total, since each gearwheel have an efficiency of 99 %, and the total efficiency of the drivetrain system is then:

$$0.99^8 = 0.92$$

The performance of this system is calculated in similar way as for the quadrotor that converts all of its mechanical energy to electrical energy.

$$Endurance = \left(5 + \frac{(121 - 5)}{0.7} \right) \cdot 0.2 + \left(5 + \frac{(121 - 5)}{0.7} \right) \cdot 0.8 \cdot \frac{0.92}{0.52} = 276 \text{ min}$$

The distance the aircraft could travel is then:

$$Distance = (276 - 5) \cdot 15 \cdot \frac{60}{1000} = 244 \text{ km}$$

The performance of this quadrotor would be quite impressive, and the endurance of this aircraft is directly comparable to LUTAB's Pegasus quadrotor. Pegasus will always be the most efficient way to fly since it is able to fly as an aircraft during its mission, with 2 kg of fuel Pegasus have an endurance of 8 h, while a quadrotor that also converts all of its mechanical energy to electrical energy have an endurance of 2.8 h. But when one chose to drive the propellers directly this change, the endurance of such aircraft is now 4.6 h, it might be a bit unfair to compare Pegasus that converts all of its mechanical energy into electrical energy with this aircraft, but converting the Pegasus into a similar directly driven system is harder and would add a significant amount of extra weight to the system. For the Pegasus solution one has assumed that the efficiency of the propeller is 0.7 and that the engine has an efficiency of 0.85, this leads to a total efficiency 0.595 for these two components. The efficiency of the MW-8R is assumed to be only 0.33 for these components. The rotor radius of the MW-8R is 0.3 m, this is a fairly large propeller which should be possible to make more efficient. If the efficiency could be made as high as for the Pegasus system the endurance would then be:

$$Endurance = 4.6 \cdot \frac{0.595}{0.33} = 8.3 \text{ h}$$

And the distance it could travel is:

$$Distance = 244 \cdot \frac{0.595}{0.33} = 440 \text{ km}$$

This means that this system is precisely as good as the Pegasus solution as long as it cannot be made into a directly driven system.

It is intended that the MW-8R should be made into a ducted fan propeller system, this would most likely further increase the performance of it, but how the induced power and flight speed is affected by a ducted fan configuration has not been investigated in this report, but it is known that the time the aircraft could spend in hover would increase dramatically. It is probable that an aircraft of this type that is intended to lift supplies should be designed as a ducted fan system since this would increase the lift significant, while the reconnaissance version might skip the ducted fan design in favor of more speed.

If the MW-8R is built it would be an exceptional reconnaissance aircraft with almost as long endurance in hover as for in loiter. Only 30 % of the power is saved by letting the aircraft loiter over the target, while Pegasus totally depends on the ability of flying with airspeed for long endurance.

Even though the engine used in this quadrotor is underpowered for the use of a quadrotor that is intended to resupply soldiers behind enemy lines, these calculations suggest that it is possible to construct such an aircraft if desired.

7. Extended sight - Demonstrator

This part of the report focuses on the work to build a demonstrator for the extended sight concept. The requirement for the demonstrator is that it should reach a height enough to clear the treetops in Swedish forests; a height of 30 m was decided to be enough. Sadly no demonstrator was built since the time available for this project ended and that one of the quadrotors available was destroyed when a 12 V battery was connected, the reason for this accident is still unknown but a possible reason is that the author of this report connected the AR.Drone to the wrong polarity on the battery even though he double checked where the cables went.

7.1 Electrical system

The first part of designing the electrical system was to find a cable suited for the application. Previous work made show that an aluminum cable is the optimal choice, but a cable that was for sale on the private market could not be found. A copper cable that is used in the windings within transformers was chosen instead. This cable have however the advantage of already being isolated. Two windings of this type of cable were bought, each winding is 40 m long, weighs 100 g, and the diameter of the cable is 6 mm.

The quadrotor draws approximately 7 A when in flight with the extra load of 200 g cable. The total resistance of 80 m of this copper cable is 5 Ω , using this cable in combination with a DC power supply of 48 V enables the quadrotor to fly 40 m up in the air (since the quadrotor needs two cables for each polarity). Equation (25) is based on ohms law and calculates the maximum current that is able to go through the circuit.

$$I = \frac{U_{battery} - U_{quad}}{R_{cable}} = \frac{48 - 11.1}{5} = 7.38 \text{ A} \quad (25)$$

Flying higher than 40 m with this cable is not possible since the resistance of the cable is increasing with the length of it, and as the resistance grows, the maximum current through the circuit decreases. This design was originally thought to be enough but since the current that the quadrotor draws is varying from 5-7 A depending on lifted cable, this will result in far varying differences in the potential at the quadrotor. When the quadrotor is consuming 5 A the potential at the end of the cable windings is:

$$U_{quad} = U_{battery} - R_{cable} \cdot I = 48 - 5 \cdot 5 = 23 \text{ V}$$

This is more than twice the potential that the electrical system is designed for. An electrical system onboard the quadrotor is therefore needed to reduce this voltage to the required 11.1 V. It was decided that this system should dissipate this extra energy as heat since making a system that transforms the potential to 11.1 V almost without losses would weigh too much for this application. The system also needs to dissipate the extra energy during the two modes of the quadrotor.

Mode 1: Startup phase, draws a current of 0.211 A. This small current would result in a potential of 47 V at the quadrotor.

Mode 2: Flight, draws 5-7 A. Results in a varying potential between 23-12 V at the quadrotor.

Figure 38 and Table 19 show the electrical scheme of the system that was designed and the specifications of the components that are used.

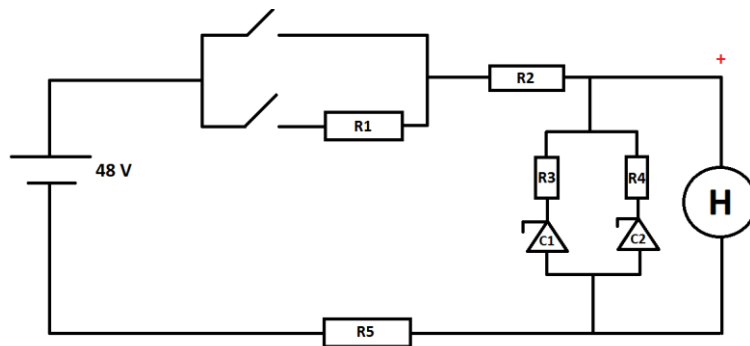


Figure 38 - Electrical scheme

Component	Specification
R1	Resistor, 75 Ω
R2	Cable winding, 2.5 Ω
R3	Resistor, 0.5 Ω
R4	Resistor, 0.5 Ω
R5	Cable winding, 2.5 Ω
C1	Zenerdiode, 12 V, 50 W, 6 g
C2	Zenerdiode, 12 V, 50 W, 6 g

Table 19 - Component specification

Two of the most powerful zenerdiodes available in parallel connection bought from the electronics company *Elfa* is chosen to dissipate the extra energy. Zenerdiodes work like a normal diode in its forward direction, but in its backward direction it's different. It permits all current going through its backward direction until the potential between the diode reaches a specific value where the diode has been designed to open. This is known as the breakdown voltage. When the potential reaches values over 12 V, the diode opens and lets current go through it, this prevents the potential to grow higher than 12 V between the diode. It is at these points between the diode that the quadrotor is connected. Two resistors have however been connected in front of each zenerdiode to prevent them to open separately due to their opening characteristics. The quadrotors Li-Po battery leaves a potential of 12.7 V when it is fully charged, this means that the system is not that sensitive for voltages slightly higher than 11.1 V that it is designed for. And since no 11.1 V zenerdiodes could be found on the market the 12 V ones are chosen instead.

Even though the zenerdiodes bought is one of the most powerful available, these are not enough to dissipate the energy required in Mode 1. The solution to this is to use two current switches, the first one is opened for Mode 1, the current is then led through a resistor of 75 Ω and most of the energy is dissipated there instead. When the startup phase of the quadrotor is done, the second current switch is turned on. It is important to liftoff as fast as possible after this is done in order to not overheat the zenerdiodes. When the quadrotor is in flight and are consuming energy, less current is flowing through the zenerdiodes and the heating of them is therefore no problem.

The part of the electrical system that has to be carried within the quadrotor is the zenerdiodes with their two small resistors; this means that the extra weight that the quadrotor has to carry is only 12 g if neglecting the weight of the resistors.

7.1.1 Testing the electrical system

The electrical system constructed should serve as a predecessor for a future one, the performance and faults of this system is stated below to help future development of the system. Figure 39 shows how the test system built looks like.

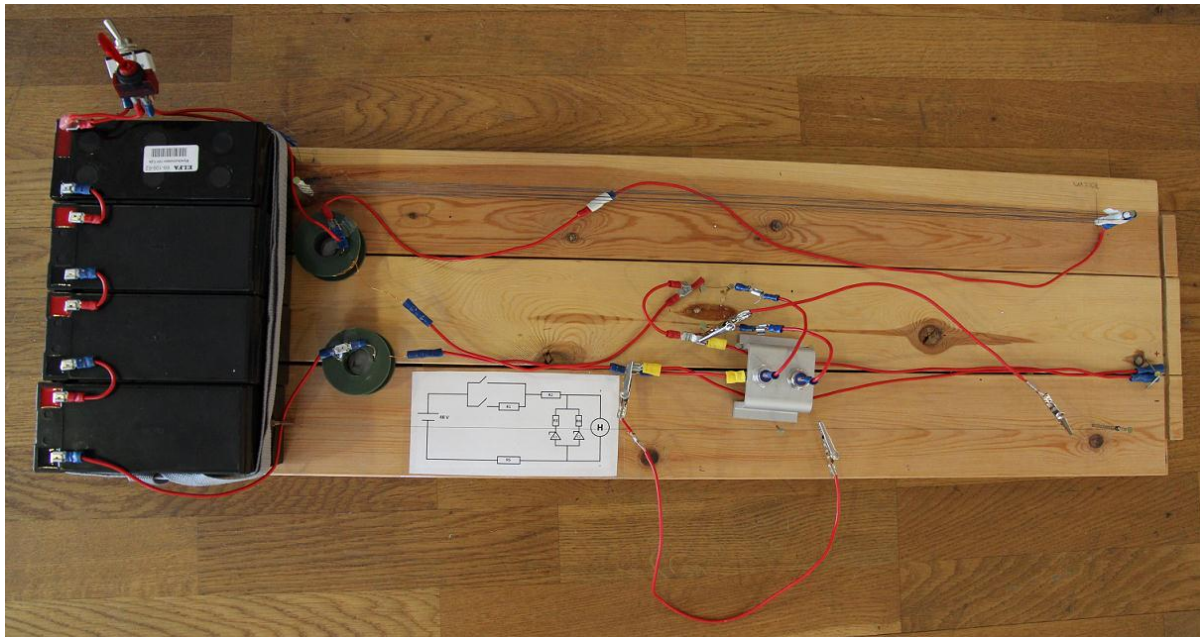


Figure 39 - Picture of the electrical system

The electrical system designed worked overall well, but it had some problems keeping a constant potential between the points that the quadrotor is connected. This problem is due to that the resistors R1 and R2 are slightly too strong which results in a potential drop over the resistor when large currents is flowing through it, this potential drop is added to the 12 V of the zener-voltage and resulted in some cases in a voltage at the quadrotor of 13.3 V. This voltage is probably no problem for the quadrotors system but this should be kept in mind when developing a future version of this electrical system.

Another problem is the heating in the copper windings; they became so hot that the plastic roll that the cable is wound upon started to melt. The heat also resulted in a continuously dropping current through the system due to the extra resistance due to heating. There is therefore a need of some kind of cooling at the windings, note that this is not a problem for the copper cables outside the windings.

7.2 Flying the AR.Drone tethered

If the extended sight concept is to be realized, one has to understand how a quadrotor behaves when tethered to a line. So some test flights had to be done to prove this concept, a description of how the test was done is followed.

To be able to attach a line to the quadrotor one hade to add some kind of attachment point on the quadrotor. There where worries that the ultrasound altimeter would detect the attachment arrangement and the line as the ground, so this might have to be avoided. Figure 40 show how the AR.Drone hovering with this attachment arrangement.



Figure 40 – Me test flying the AR.Drone indoors with its attachment arrangement

The AR.Drone was first flown with this arrangement indoors and the quadrotor had no problems in maintaining its altitude despite the potential risk of this arrangement jamming the ultrasound altimeter. The quadrotor was then flown outside tethered to a fishing line wound upon an ice fishing rod. Figure 41 shows Owe Lyrsell holding the AR.Drone and the ice fishing rod.



Figure 41 - Owe Lyrsell holding the AR.Drone and a fishing rod

When the quadrotor first flew outside, it could not fly higher than 3 m due to a built in altitude limitation in the software. This feature was switched off and the quadrotor was now able to fly without limitations. The quadrotor flew quite well if the fishing line was hanging almost straight down to the ground, one could tension the fishing line and pull it in different directions without crashing the AR.Drone. But when the line that was connected to the quadrotor was not hanging straight down to the ground, this changed. When this happened in combination with the line being stretched, the quadrotor got unstable and crashed. This unwanted effect had to do with how the line was attached to the quadrotor, when the line got stretched in this situation it resulted in that one or two of the four white lines that the attachment arrangement consisted of got stretched, this pulled down the quadrotor in a circle with the same radius as the length of the line. The solution to this problem was to redo the attachment; the new attachment can be seen in Figure 42.



Figure 42 - New attachment arrangement

With this new attachment arrangement the quadrotor flew well without crashing, it was now time to test how the AR.Drone would fly with a more heavy cable. The cable that was used consisted of two transformer cables that were taped together, which is the suggested cable to supply the demonstrator with power. No current was however run through the cables so the quadrotor had to fly on its batteries instead, this meant that the quadrotor had to lift both the cable and the weight of the battery, which affects the total height achievable. Figure 43 shows the AR.Drone flying with a power supply cable connected to this new attachment arrangement.

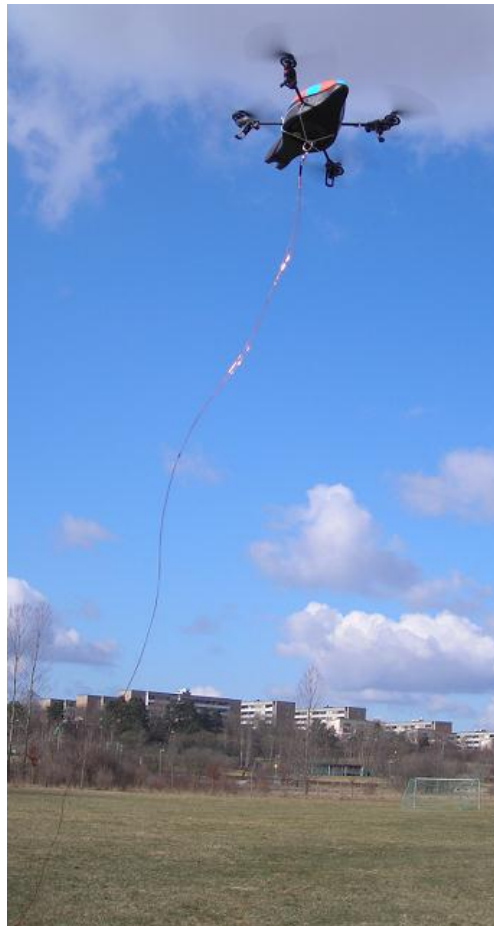


Figure 43 - AR.Drone in the air with its new attachment arrangement connected to a power supply cable

The test flights with this new arrangement and the power cable attached was successful, the quadrotor flew stable in the air even though the wind speed was as high as 7 m/s. It reached a height of about 15 m under these conditions; this suggests that the quadrotor should be able to reach a height of 40 m without the extra weight of the battery. The weight of the cable does somewhat change the quadrotor's center of gravity downwards and the effect of this should be investigated for a future heavier tank version of the extended sight concept even though having a low center of gravity usually tends to stabilize vehicles.

8. Conclusion

The extended sight concept seems promising and actual for the time being. The main problem for this system is the loss in the power supply cable which leads to high energy consumption and large potential differences at the aircraft which must be converted into the right magnitude. A solution to this problem has been constructed and tested with promising results. It is also shown that by just choosing the right potential to power the extended sight quadrotor could reduce the power loss in the cable significantly and therefore increase the length of the cable, and that wind blowing on this cable will result in an altitude loss for the extended sight quadrotor. A demonstrator for this concept has been started to be built but couldn't be finished due to lack of time.

Investigations show that battery powered quadrotors have an optimal size for a given requirement and that the performance drops if one constructs a bigger or smaller quadrotor. Same investigations show that micro quadrotors would be the best performing ones in terms of obtaining the longest endurance.

A number of suggestions for improvements to the quadrotor platform have been proposed; the most promising one is the use of ducted fan propeller system which could in theory increase the time that the quadrotor could spend in hover by a factor of three.

Further investigations show that a hybrid quadrotor with an 1154 W engine would be able to maintain itself in hover for about 2-3 h depending on payload. In this report a suggestion of an improved design of such quadrotor called MW-8R has been proposed that has promising performance in theory. If built this quadrotor would give the military a long endurance reconnaissance UAV with VTOL capability.

Investigations done under this subject suggest that the military would benefit from having quadrotors in their arsenal. The use that the military could have from quadrotors is mainly for the purpose of reconnaissance, but combustion based systems could carry enough payload to resupply soldiers or place out surveillance equipment far behind enemy lines.

9. Recommendations for future work

There is some remaining work left to do in order to gain enough information to be able to fully understand the potential of the quadrotor platform from a military point of view. This chapter contains suggestions for future work on this subject.

9.1 Ducted fan quadrotor

It is already known that a ducted fan configuration would improve the performance of an extended sight quadrotor significant by allowing one to use longer cables. But when one is to design a quadrotor for reconnaissance, one needs to know if the ducted fan quadrotor is to be preferred or not. There is a company that has produced a ducted fan quadrotor [10], but data of its flight performance is very scarce. An independent source on the internet claim that they have improved the quadrotors efficiency by 33 % but none of this information is available on the manufacturer's web page. Figure 44 show the only found commercial ducted fan quadrotor.



Figure 44 – Cyber-technology's CyberQuad

If one modifies the AR.Drone into a ducted fan configuration one could test its performance compared to the original version. A duct has already been constructed for this report so little work remains to convert the AR.Drone into a ducted fan system. The author suspects that it is due to the large rotor diameter helicopters don't use ducts. Tests are to be done to measure the power consumption of a ducted fan quadrotor both in hover and translation flight and compare these data with the original version. The induced power of the two quadrotors is also to be measured to get a better understanding of how the duct affects the induced power.

9.2 Finalize and test the extended sight demonstrator

Almost all work has been done in order to get AR.Drone extended sight demonstrator in the air, the work left is to build in the electrical system into the quadrotor and construct some kind of cooling device for the copper windings. Then one could start to test the potential of this concept. Test should also be done to see how a low center of gravity affects a quadrotor.

9.3 Build MW-8R

Calculations on the MW-8R concept show that it has promising performance; it is possible to build and test the MW-8R using COTS equipment such as ESC for quadrotors and other RC-equipment.

9.4 Gyroscopes potential

Gyroscopes have been mentioned a lot in this report for two main reasons, the first is to stabilize the platform or the camera with the goal to get better image quality, and the latter is to control the platforms attitude in same way as many satellites do in space. A suggestion for work regarding this concept is to build a light moment wheel and place it into the AR.Drone, then fly the quadrotor into the slipstream from a fan and see if it becomes more stabilized than a quadrotor without this gyroscope. If the results are promising with respect to improved stability of the platform and better image quality, one can start testing if it is possible to control the quadrotors attitude using this equipment. This could be done by using the same moment wheel and place it on a movable surface in the quadrotor that can tilt this wheel in different directions, if the quadrotor changes attitude in a satisfactorily way one could argue for that gyroscopes is a good way of controlling and stabilizing UAV aircraft. If the gyroscope concept proves to be satisfying and

FMV wants to continue the work on the extended sight concept, one should consider building the alternative solution for the extended sight concept in section 4.2.7. One should also investigate the image quality of cameras mounted on UAV's that have built in gyroscopes and compared them with cameras that without to fully understand the potential of using gyroscopes on UAV's. Tests could also be made to see if a gyroscope might be able to reduce the power consumption of a quadrotor due to reducing the need for accelerating the engines in order to balance the quadrotor.

9.5 Efficiency of propellers and engines

The static thrust producing propellers available on the market have a low value on their efficiency, investigations could be made to discover why these propellers have so low efficiency. It might be the case that most RC-aircraft propellers on the market are not optimized to produce static thrust. One should also investigate how the efficiency of the propeller and the engine grows with increased size to better understand how large one should build a quadrotor. When this information is gained it is to be implemented in the flight time approximation model and recommendations of how to size a quadrotors that are supposed to carry different payloads is to be made.

9.6 Evasive maneuver programming

If *FMV* are interested in continuing the work on the extended sight concept one could make a program to the AR.Drone that demonstrates the evasive maneuvering system. When this is done one can calculate how much the risk that the quadrotor is being hit is reduced, when being fired upon with various weapons at different distances.

9.7 Indoor reconnaissance programming

As mentioned in section 3.4, the AR.Drone has difficulties holding its position in indoor flight, this problem increases when flying over object such as chairs. A program could therefore be made to improve the AR.Drone's ability to operate indoors, if the sensors onboard are the limiting factors one could try to upgrade them.

10. References

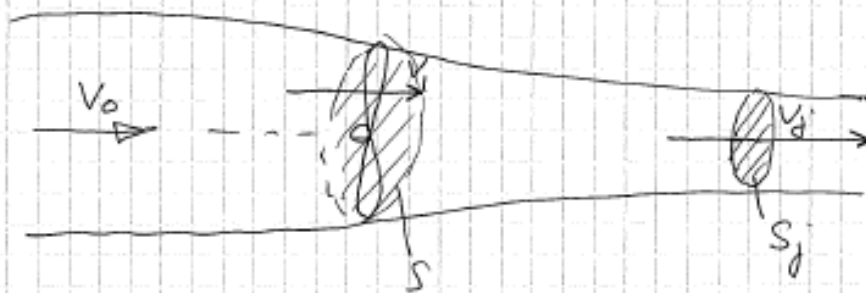
- Ref [1] J. G. Leishman, *Principles of Helicopter Aerodynamics*, pp. 36-71, Cambridge University Press, 2000
- Ref [2] Will E. Graf, *Effects of Duct Lip Shaping and Various Control Devices on the Hover and Forward Flight Performance of Ducted Fan UAVs*, pp. 6, http://www.dept.aoe.vt.edu/~mason/Mason_f/WillGrafMSThesis.pdf, 2005
- Ref [3] Owe Lyrsell & Mattias Björk, *UAV with enhanced capabilities, summary report (PEGASUS)*, LUTAB, 2011
- Ref [4] Anita I. Abrego & Robert W. Bulaga, *Performance Study of a Ducted Fan System*, American Helicopter Society International, 2002
- Ref [5] Mikhail Sharonov, *AR.Drone Diagnostics*, <http://www.msh-tools.com/ardrone/>, 2011
- Ref [6] Haomiao Huang, *Aerodynamics and Control of Autonomous Quadrotor Helicopters in Aggressive Maneuvering*, Stanford University, 2009
- Ref [7] Young & Freedman, *Sears and Zemansky's University physics*, Addison Wesley, 2008
- Ref [8] Wayne Johnson, *Helicopter Theory*, pp. 128, Princeton University Press, 1980
- Ref [9] Draganflyer X8, <http://www.draganfly.com/uav-helicopter/draganflyer-x8/index.php>
- Ref [10] CyberQuad, <http://www.cybertechuav.com.au/-Overview,85-.html>

Appendix A – Propeller theory

E. Preisell

1(2)

Propellerteori



$$\begin{cases} S = \text{diskarea (m}^2\text{)} \\ S_j = \text{Slipström rörsarea (m}^2\text{)} \end{cases} \begin{cases} V_0 = \text{flyghastighet (m/s)} \\ V_1 = \text{hastighet genom propellerdisk (m/s)} \\ V_j = \text{Slipströmhastighet} \end{cases}$$

$$V_j > V_1 > V_0$$

$$\begin{cases} T_s = \text{statisk dragkraft (N)} \\ \dot{m} = \text{massflöde (kg/s)} \\ \rho = \text{densitet (kg/m}^3\text{)} \\ P = \text{Effekt (W)} \end{cases}$$

" T_s " Statisk dragkraft $V_0 = 0$

$$T_s = \dot{m} \cdot V_j = \rho V_j \cdot S_j \cdot V_j = \rho S_j \cdot V_j^2$$

$$V_j = \sqrt{\frac{T_s}{\rho S_j}} \quad \dots (1)$$

$$P = \dot{m} \cdot \frac{V_j^2}{2} = \rho V_j S_j \cdot \frac{V_j^2}{2} = \rho S_j \cdot \frac{V_j^3}{2}$$

$$V_j = \sqrt[3]{\frac{2P}{\rho S_j}} \quad \dots (2)$$

[Signature]

Appendix A – Propeller theory

2(2)

$$(1) = (2)$$

$$\sqrt{\frac{T_s}{\rho S_j}} = \sqrt[3]{\frac{2P}{\rho S_j}}$$

$$\frac{T_s}{\rho S_j} = \left(\frac{2P}{\rho S_j} \right)^{2/3}$$

$$\Rightarrow T_s = \sqrt[3]{4 \cdot P^2 \cdot \rho \cdot S_j} \quad \text{--- (3)}$$

$$\Rightarrow P = \frac{T_s^{3/2}}{2\sqrt{\rho S_j}} \quad \text{--- (4)}$$

Men statistiskt är $V_j = 2V_i$ dvs $S_j = \frac{S}{2}$

$$\Rightarrow P = \frac{T_s^{3/2}}{\sqrt{2\rho S}} \quad \text{--- (5)}$$

Dessa är ideala samband. I verkligheten!

$$T_s = K \cdot \sqrt[3]{2P^2 \cdot \rho \cdot S} \quad \text{--- (3'')}$$

$$P = \left(\frac{1}{K} \right)^{3/2} \frac{T_s^{3/2}}{\sqrt{2\rho S}} \quad \text{--- (5'')}$$

$K \approx 0,5$ för en högt belastad propeller

$K \approx 0,6$ för en lågt belastad propeller

$$\text{Ex. } K=0,5 \quad \left(\frac{1}{K} \right)^{3/2} \approx \underline{\underline{2,83}}$$



Appendix B – AR.Drone system specifications

EMBEDDED COMPUTER SYSTEM

- Processor: ARM9, 32 BITS, 468 MHz
- Memory: DDR RAM, 128 Mb, 200MHz
- Data transfer: Wi-Fi b/g, USB
- Operating system: Linux OS

INERTIAL GUIDANCE SYSTEMS WITH MEMS

- 3-axis accelerometer
- 2-axis gyrometer
- 1-axis yaw precision gyrometer

SAFETY SYSTEM

- EPP hull for indoor flight
- Automatic locking of propellers in the event of contact
- UL2054 battery
- Control interface with emergency button to stop the motors

AERONAUTIC STRUCTURE

- High-efficiency propellers (specially designed for the Parrot AR.Drone)
- Carbon-fiber tube structure

ULTRASOUND ALTIMETER

- Emission frequency: - 40kHz
- Range 6 meters, used for vertical stabilization

MOTORS AND ENERGY

- 4 brushless motors, (35,000 rpm, power: 15W)
- Lithium polymer battery (3 cells, 11 V, 1000 mAh)
- Discharge capacity: 10C
- Battery charging time: 90 minutes

FRONT CAMERA: WIDE ANGLE CAMERA

- 93° wide-angle diagonal lens camera, CMOS sensor
- Encoding and live streaming of images on iPhone
- Camera resolution 640x480 pixels (VGA)
Other AR.Drone detection
 - Validation of shots fired at enemy drones
 - Estimate of distance
 - Detection distance: 5 meters3D tag detection
 - Positioning of virtual objects
 - Calculation of markers of virtual objects
 - Detection distance: 30 centimeters to 5 meters
- Video feedback on the iPod touch /iPhone screen

VERTICAL CAMERA: HIGH SPEED CAMERA

- 64° diagonal lens, CMOS sensor
- Video frequency: 60 fps
- Allows stabilization even with a light wind

Appendix C – Measurements on AR.Drone's propulsion system made by Airspeed Industry

Delrapport 1, Dragkraft och energimätningar på Quadrocoptermotorinstallation.

Förutsättningar för mätningarna:

Proven syftar till att ge nödvändigt underlag för X-jobbare Mathias Wennbergs studie av en Quadrocopter av fabrikat Parrot drone.

Utrustning:

En Parrot drone har modifierats genom att en enskild motor med växellåda har galvaniskt frånskilts från den vanliga reglerelektroniken. Som ersättare för detta har ett normalt fartreglage för modellflyg installerats.

Reglagetyp: Swift. För upp till 3 celler LiPo och max 10A. Förlusterna i detta reglage är mycket ringa.

Dronen har sedan monterats på en dragkraftsvåg med en utväxling på 3,68:1. Denna installation har tidigare använts för FMVs prov av "Coandafarkost" och kunde för att spara tid modifierats för detta prov. Den digitala vågen som använts är av fabrikat Radwag med en nogranhet på 0,1gram.

Som energikälla har ett 3-cells LiPo paket använts, fabrikat Arrowind. Detta högprestandapaket valdes då det tål en kontinuerlig urladdning på 77 Ampere varför något spänningsfall inte behövdes tas hänsyn till under mätningarna. Spänningen var konstant 12,1 Volt under hela provet.

Det installerade fartreglaget reglerades via en servotester av fabrikat HitechHFP-10. Denna visar pulståglängden digitalt varför största noggrannhet och stabilitet vid regleringen kunde uppnås.

För strömmätningen användes en tysk precisionsmätare avsedd för solcellsinstallationer av typen RE-830B.

Genomförande

Hela systemet varmkördes i ca 5 minuter innan några värden registrerades. Detta för att plocka udden av batteriets toppspänning när det är färskt från laddning. Mätningarna startade sedan med 0,5A och dragkraften noterades. Mätningarna gjordes i steg om 0,5A ända upp till fullgas vilket var 3,5A. Efter detta repeterades mätningen igen för att kontrollera repeterbarheten i mätutrustningen. Inga anmärkningsvärda avvikelser förekom.

Appendix D – AR.Drone ducted fan measurements

Delrapport 2, Dragkraft och energimätningar på Quadrocoptermotorinstallation med intagsläpp.

Förutsättningar för mätningarna:

Proven syftar till att ge nödvändigt underlag för X-jobbare Mathias Wennbergs studie av en Quadrocopter av fabrikat Parrot drone.

Utrustning:

En Parrot drone har modifierats genom att en enskild motor med växellåda har galvaniskt frånskilts från den vanliga reglerelektroniken vid ett tidigare prov. Som ersättare för detta har ett normalt fartreglage för modellflyg installerats.

Reglagetyp: Swift. För upp till 3 celler LiPo och max 10A. Förlusterna i detta reglage är mycket ringa.

Intagsläpp och dysa: För detta andra prov har en dysa med intagsläpp monterats. Radien på läppen är ca 20mm och dysans parallella längd är 60mm. Propellerns placering är strax under läppens slut.

Dronen har sedan tidigare monterats på en dragkraftsvåg med en utväxling på 3,68:1. Denna installation har tidigare använts för FMVs prov av "Coandafarkost" och kunde för att spara tid modifierats för detta prov. Den digitala vågen som använts är av fabrikat Radwag med en nogranhet på 0,1gram. Installationen är inte rörd sedan det inledande provet utan intagsläpp.

Som energikälla har ett 3-cells LiPo paket använts, fabrikat Arrowind. Detta högprestandapaket valdes då det tål en kontinuerlig urladdning på 77 Ampere varför något spänningsfall inte behövdes tas hänsyn till under mätningarna. Spänningen var konstant 12,1 Volt under hela provet.

Det installerade fartreglaget reglerades via en servotester av fabrikat HitecHFP-10. Denna visar pulståglängden digitalt varför största noggrannhet och stabilitet vid regleringen kunde uppnås.

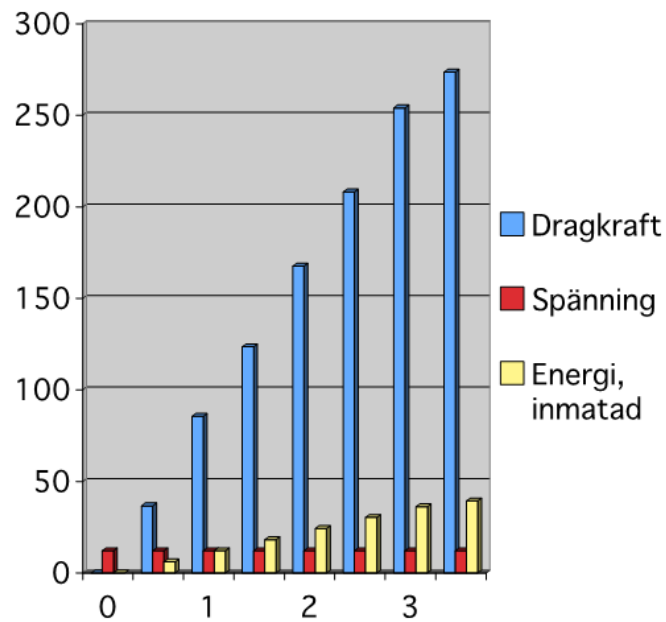
För strömmätningen användes en tysk precisionsmätare avsedd för solcellsinstallationer av typen RE-830B.

Genomförande

Hela systemet varmkördes i ca 5 minuter innan några värden registrerades. Detta för att plocka udden av batteriets toppspänning när det är färskt från laddning. Mätningarna startade sedan med 0,5A och dragkraften noterades. Mätningarna gjordes i steg om 0,5A ända upp till fullgas vilket var 3,25A (jämför med 3,5A utan dysa). Efter detta repeterades mätningen igen för att kontrollera repeterbarheten i mätutrustningen. Inga anmärkningsvärda avvikelser förekom.

Appendix D – AR.Drone ducted fan measurements

Resultat



Dragkraft-inmatad energi.

Ström (A)	0,09	0,5	1	1,5	2	2,5	3	3,25
Dragkraft (g)	0	36,7	85,6	123,6	167,7	208,2	254,1	273,6
Inmatad energi (W)	1,1	6,05	12,1	18,15	24,2	30,25	36,3	39,3
Spänning	12,2	12,1	12,1	12,1	12,1	12,1	12,1	12,1